

1
2
3
4
5
6
7
8
9
10
11
12
13
14
15
16
17
18
19
20
21
22

**Genetic control of the error-prone repair of a chromosomal double-strand break
with 5' overhangs in yeast**

Samantha Shaltz and Sue Jinks-Robertson

Department of Molecular Genetics and Microbiology, Duke University, Durham, NC 27710

Corresponding author:

Sue Jinks-Robertson

Department of Molecular Genetics and Microbiology

213 Research Drive, CARL 384

Duke University Medical Center

Durham, NC 27710

sue.robertson@duke.edu

Running head: Error-prone repair of a ZFN-induced DSB in yeast

Keywords: DSB repair, NHEJ, MMEJ, ZFN, yeast

23 **ABSTRACT**

24 A targeted double-strand break introduced into the genome of *Saccharomyces cerevisiae* is
25 repaired by the relatively error-prone nonhomologous-end joining (NHEJ) pathway when
26 homologous recombination is not an option. A ZFN cleavage site was inserted out-of-frame into
27 the *LYS2* locus of a haploid yeast strain to study the genetic control of NHEJ when the ends
28 contain 5' overhangs. Repair events that destroyed the cleavage site were identified either as
29 *Lys*⁺ colonies on selective medium or as surviving colonies on rich medium. Junction sequences
30 in *Lys*⁺ events solely reflected NHEJ and were influenced by the nuclease activity of Mre11 as
31 well as by the presence/absence of the NHEJ-specific polymerase Pol4 and the translesion-
32 synthesis DNA polymerases Pol ζ and Pol η . Although most NHEJ events were dependent on
33 Pol4, a 29-bp deletion with endpoints in 3-bp repeats was an exception. The Pol4-independent
34 deletion required TLS polymerases as well as the exonuclease activity of the replicative Pol
35 δ DNA polymerase. Survivors were equally split between NHEJ events and 1 kb or 11 kb
36 deletions that reflected microhomology-mediated end joining (MMEJ). MMEJ events required
37 the processive resection activity of Exo1/Sgs1, but there unexpectedly was no dependence on
38 the Rad1-Rad10 endonuclease for the removal of presumptive 3' tails. Finally, NHEJ was more
39 efficient in non-growing than in growing cells and was most efficient in G0 cells. These studies
40 provide novel insight into the flexibility and complexity of error-prone DSB repair in yeast.

41 INTRODUCTION

42 DNA double-strand breaks (DSBs) are potentially toxic lesions that are repaired either by
43 homologous recombination (HR), which uses an intact duplex as a template to restore the
44 broken region, or by nonhomologous end joining (NHEJ), which directly ligates broken ends
45 back together. In general, NHEJ is a more error-prone process, with out-of-register annealing
46 between ends and/or end processing creating joints with small insertions or deletions. In
47 addition, the rejoining of ends from different breaks can generate various types of genome
48 rearrangements and has been implicated in recurrent oncogenic translocations. Although most
49 DSBs are pathological and reflect either replication fork collapse, abortive topoisomerase
50 reactions or DNA damage, programmed DSBs breaks are essential in some biological
51 processes. During meiosis, for example, the Spo11 protein creates DSBs that initiate the HR
52 necessary for creating genetic diversity and for ensuring proper chromosome segregation
53 (KEENEY 2008). In mitosis, mating-type switching is initiated by the HO endonuclease in yeast
54 (HABER 2012) and RAG proteins create DSBs that initiate the NHEJ-mediated joining of
55 immunoglobulin gene segments in vertebrates (JUNG *et al.* 2006).

56 DSB repair pathways are highly conserved, and the yeast *Saccharomyces cerevisiae*
57 has served as a model for defining relevant proteins and molecular mechanisms. Broken ends
58 of all types are bound by the Ku (Ku70-Ku80) and MRX (Mre11-Rad50-Xrs2) complexes; both
59 are absolutely required for NHEJ in yeast (DALEY *et al.* 2005b). Although not required for HR,
60 MRX accelerates the initiation of 5'-end resection, which creates a 3' tail that invades an
61 homologous template and initiates HR (reviewed in SYMINGTON 2016; REGINATO AND CEJKA
62 2020). As part of the MRX complex, Mre11 nicks the 5' terminated strand and subsequent 3'>5'
63 resection towards the break generates a free 3' end. MRX activity is particularly important for
64 eliminating end-attached proteins or terminal DNA damage and additionally removes Ku from
65 ends to prevent NHEJ. In addition to its role in short-range resection, MRX facilitates the loading

66 of long-range resection activities (Exo1 and Sgs1-Dna2) to promote efficient HR. HR requires a
67 large suite of proteins to invade/copy the repair template as well as to resolve intermediates into
68 final products (reviewed in SYMINGTON *et al.* 2014). In addition to Ku and MRX, NHEJ in yeast
69 requires the dedicated Dnl4 DNA ligase (TEO AND JACKSON 1997) and the Pol4 DNA
70 polymerase (WILSON AND LIEBER 1999).

71 Early NHEJ studies in yeast used transformation-based assays to assess the closure
72 efficiency of linearized plasmids with defined end structures and to molecularly define the
73 ligated products (reviewed in DALEY *et al.* 2005b). An advantage of this type of system is that
74 end sequence can be manipulated *in vitro* to yield completely or partially complementary ends,
75 or to generate completely incompatible ends (e.g., blunt ends or ends with different polarity).
76 With ends that have complementarity, the default is simple re-ligation. Following the annealing
77 of ends with partial complementarity, gaps flanking the annealed region must be filled before
78 ligation occurs. With 5' overhangs, the filling of associated gaps is primed from a stably base-
79 paired 3' end. With 3' overhangs, however, gap filling must occur from a 3' end stabilized by at
80 most a few base pairs and is more dependent on Pol4 (DALEY *et al.* 2005a). In contrast to 3'
81 overhangs, the recessed 3' ends of 5' overhangs can directly be extended in the absence of
82 end annealing. With overhangs that lack complementarity or are incompatible, joining usually
83 involves processing-uncovered microhomologies that flank the broken ends.

84 Mitotic studies of DSB repair in a chromosomal context have relied on endonucleases
85 that create a single, targeted DSB and repair is monitored through selection of survivors or
86 prototrophs. HO or I-SceI, which generate breaks with 4-nt 3' overhangs had been used
87 extensively to study error-prone DSB repair (e.g. VILLARREAL *et al.* 2012; DENG *et al.* 2014). Zinc
88 Finger Nucleases (ZFNs), which create 4-nt 5' overhangs, and Cas9, which mostly creates blunt
89 ends, have only rarely been used (LIANG *et al.* 2016; LEMOS *et al.* 2018; SHALTZ AND JINKS-
90 ROBERTSON 2021). Because *S. cerevisiae* relies mainly on HR for the repair of genomic DSBs,

91 NHEJ following endonuclease cleavage is studied either in the absence of a repair template or
92 by disabling recombination. Precise rejoining of the ends by the NHEJ machinery regenerates
93 the cleavage site, resulting in repetitive cycles of cleavage-ligation until a rare error-prone event
94 renders the target sequence refractory to cleavage. Error-prone NHEJ typically involves minor
95 addition or deletion of sequence from the broken ends and often reflects the annealing of small
96 microhomologies within the overhangs, although microhomology is not a requirement. The
97 overhang sequence dictates the spectrum of insertions/deletions and this sequence cannot be
98 varied when DSBs are initiated with I-SceI or HO. By contrast, use of a ZFN to create a DSB
99 allows manipulation of the 5' overhang sequence (LIANG *et al.* 2016; SHALTZ AND JINKS-
100 ROBERTSON 2021). Reflecting the different reactions that can occur at 5' versus 3' overhangs,
101 the kinetics and fidelity of repair also differ (LIANG *et al.* 2016).

102 In addition to the classical NHEJ pathway, yeast has an alternative end-joining pathway
103 that is referred to as microhomology-mediated end joining (MMEJ). MMEJ is characterized by
104 its Ku independence and a requirement for 6-14 bp of microhomology (reviewed in SFEIR AND
105 SYMINGTON 2015). Finally, single-strand annealing (SSA) requires more extensive homology
106 between direct repeats and is usually considered a variant of HR. In contrast to the canonical
107 HR pathway, however, SSA is independent of the Rad51 strand-invasion protein (IVANOV *et al.*
108 1996), as is MMEJ (LEE AND LEE 2007). The transition from MMEJ to SSA occurs when the
109 microhomology reaches 15-20 bp and SSA, but not MMEJ, has strong dependency on the
110 Rad52 strand-annealing protein (VILLARREAL *et al.* 2012). It should be noted that higher
111 eukaryotes lack a yeast-like MMEJ pathway and instead have an alternative end-joining
112 pathway that is mediated by the Pol theta DNA polymerase (SFEIR AND SYMINGTON 2015).

113 We previously described a system that used a galactose-induced ZFN to create a site-
114 specific DSB in the yeast *LYS2* gene (SHALTZ AND JINKS-ROBERTSON 2021). Insertion of an out-
115 of-frame cleavage site allowed either the selection of NHEJ-mediated repair events that

116 restored *LYS2* function or of repair events that simply allowed survival. Approximately half of the
117 latter were Ku-independent MMEJ events (SHALTZ AND JINKS-ROBERTSON 2021). In the current
118 study, this system was used to explore the genetic control of NHEJ- and MMEJ-mediated repair
119 events.

120

121

122 **MATERIALS AND METHODS**

123 ***Media and Growth Conditions***

124 All growth of yeast strains was at 30°C. For ZFN induction, cultures were grown non-
125 selectively in YEP (1% yeast extract, 2% Bacto-peptone, 300 mg/liter adenine) supplemented
126 with 2% raffinose (YEPR). Continuous ZFN expression was achieved by plating appropriate
127 dilutions onto non-selective YEPGal, which contained 2% galactose, or onto selective SGal-lys
128 synthetic medium (1.7 g/liter yeast nitrogen base, 0.5% ammonium sulfate, 2% agar, 2%
129 galactose; all amino acids and bases except lysine). The total number of cells at the time of
130 plating on galactose medium was determined by plating an appropriate dilution on YEPD
131 medium (YEP plus 2% dextrose). Following transformation during strain constructions, selection
132 was on YEPD containing the relevant drug or on synthetic medium missing the appropriate
133 amino acid or base. Ura⁻ derivatives during two-step allele replacement were selected on
134 synthetic medium supplemented with 5-fluoroorotic acid. Phenotypes following tetrad
135 dissections were determined by replica-plating onto appropriate media. All mutant genotypes
136 were confirmed by PCR.

137

138 ***Strain constructions***

139 All strains used were derived from the W303 background (*leu2-3,112 his3-11,15 trp1-1*
140 *ura3 ade2-1 CAN1 RAD5*) either by transformation or by mating and tetrad dissection. Each
141 strain contained a galactose-inducible ZFN designed to cleave the *Drosophila rosy* locus

142 (BEUMER *et al.* 2006) and a *lys2* frameshift allele containing a ZFN cleavage site. Genes
143 encoding the ZFN constituent proteins RyA and RyB were integrated into the yeast as
144 previously described (SHALTZ AND JINKS-ROBERTSON 2021) and ZFN cleavage sites were
145 introduced into the *LYS2* locus using the *delitto perfetto* method (STORICI AND RESNICK 2006).
146 Gene-deletion derivatives of SJR4848 were derived by one-step allele replacement using a
147 plasmid-derived PCR cassette containing a selectable marker. The selectable cassettes used
148 were *loxP-hphMX-loxP* from pSR955 (CHO AND JINKS-ROBERTSON 2019), *loxP-natMX-loxP* from
149 pAG25 (GOLDSTEIN AND MCCUSKER 1999), *loxP-URA3KI-loxP* from pUG72 and *loxP-TRP1-loxP*
150 from pSR954 (CHO AND JINKS-ROBERTSON 2019). The *pol4-D367E* or *rev3-D975A* allele was
151 introduced using *delitto perfetto*; the *mre11-D56N* or *pol3-DV* allele was introduced by two-step
152 allele replacement using plasmid pSM444 (LLORENTE AND SYMINGTON 2004) or pY19 (JIN *et al.*
153 2001), respectively.

154

155 **Mutation Frequencies and Spectra**

156 Independent cultures were grown in YEPR to an optical density (OD) reached 0.3-0.6,
157 at which point appropriate dilutions of “growing” cells were plated on YEPD to determine total
158 cell number, on YEPGal to select survivors of continuous ZFN expression or on SGal-lys to
159 select Lys⁺ revertants. To obtain a non-growing population of cells, incubation was continued for
160 an additional day. G0 cells were isolated following the incubation of 25 ml YEPR cultures for
161 seven days; small, unbudded G0 cells were obtained from the supernatant following low-speed
162 centrifugation (KOZMIN AND JINKS-ROBERTSON 2013). The 95% confidence interval (CI) of the
163 Lys⁺ frequency in each background was calculated using the standard error of the mean. Only
164 “corrected” survival frequencies, which correspond to error-prone repair following continuous
165 ZFN expression, are reported here and each was calculated by multiplying mean survival
166 frequency on YEPGal by the fraction of sequenced colonies in the corresponding spectrum that
167 had lost the ZFN cleavage site. The 95% CI for each corrected survival frequency was

168 calculated by combining the 95% confidence interval for the measured frequency with the 95%
169 CI for the proportion of sequenced colonies that had lost the ZFN cleavage site (MOORE *et al.*
170 2018). Frequencies of revertants and survivors in all backgrounds analyzed are in Table S1.

171 Mutation spectra in revertants and survivors were obtained by sequencing (Sanger
172 method) a PCR-generated fragment spanning the ZFN recognition site. PCR failure was
173 diagnostic of a large deletion that removed one or both of the primer-binding sites. The identity
174 of the deletion was confirmed using a different set of primers, followed by sequencing the
175 product (SHALTZ AND JINKS-ROBERTSON 2021). Complete spectra in revertants and survivors in
176 all genetic backgrounds analyzed are in Table S2 and Table S3, respectively. The distributions
177 of mutation types in different genetic backgrounds were compared using a global Chi-square
178 test (Vassarstats.net). When a significant P value was obtained ($p < 0.05$) comparisons of
179 individual mutation types were then done and the P value for significance was adjusted by
180 dividing 0.05 by the total number of comparisons performed (Bonferroni correction).

181

182

183 **RESULTS AND DISCUSSION**

184 A galactose-regulated, heterodimeric ZFN designed to cleave the *Drosophila rosy* locus
185 (BEUMER *et al.* 2006) was used to introduce a site-specific DSB in the *LYS2* gene (SHALTZ AND
186 JINKS-ROBERTSON 2021). Each ZFN subunit contained three zinc fingers and recognized a 9-bp
187 target sequence flanking a spacer of sequence 5'-ACGAAT (Figure 1A). Insertion of the 24-bp
188 *rosy* target into *LYS2* created a -1 frameshift allele and net +1 mutations that restored the
189 correct reading frame were selected by plating exponentially growing cultures on lysine-deficient
190 medium containing galactose. Selection of surviving colonies on galactose-containing rich
191 medium allowed a relatively unbiased assessment of events that eliminated the ZFN cleavage
192 site. The genetic control of revertants, which reflected canonical NHEJ, and survivors, which
193 reflected both NHEJ and MMEJ events, are described below.

194

195 **Effects of core NHEJ components on ZFN-induced Lys⁺ revertants**

196 In a wild-type (WT) background, the frequency of Lys⁺ prototrophs was 2.03 x10⁻⁴
197 (Figure 2A) and there were three major classes of NHEJ events, each of which accounted for
198 approximately 30% of revertants (Figure 2B; SHALTZ AND JINKS-ROBERTSON 2021). The first
199 class (69/226) had a CGAA insertion (+CGAA) resulting from the complete fill in of each of the
200 ZFN-generated 5' overhangs (Figure 1B). The second major class (59/226) contained a 2A>3A
201 expansion that is most easily explained by mis-annealing of the overhangs, followed by end
202 trimming, gap filling and ligation. In the third class of Lys⁺ revertants (61/226) there was
203 expansion to two thymines of a single thymine located immediately adjacent to the downstream
204 ZFN-created overhang. We previously suggested that the 1T>2T event reflects misincorporation
205 of an adenine, followed by realignment/slippage that regenerates the 4-nt overhang for direct
206 ligation. Among the remaining events was a recurrent 29-bp deletion with endpoints in a GCC
207 repeat (4/226; Figure 1C) as well as a variety of other minority events (33/226; see Table S2).

208 We previously reported that the frequency of Lys⁺ revertants decreased four orders of
209 magnitude in a *yku70Δ* background (SHALTZ AND JINKS-ROBERTSON 2021) and we observed a
210 similar reduction in *dnl4Δ* and *mre11Δ* strains (Table S1). Although Mre11 is required for NHEJ
211 in yeast (MA *et al.* 2003), loss of only its nuclease activity stimulates NHEJ-mediated repair of 3'
212 overhangs, presumably by slowing initiation of the processive 5' end resection required for HR
213 (LEE AND LEE 2007; DENG *et al.* 2014). Introduction of the nuclease-dead *mre11-D56N* allele
214 (MOREAU *et al.* 1999) into the ZFN system similarly stimulated Lys⁺ revertants 8-fold (Figure 2A)
215 but additionally was associated with an unanticipated change in the spectrum of NHEJ events
216 (Figure 2B; p<0.0001). Thus, in addition to a general repressive effect on NHEJ, Mre11
217 nuclease activity altered molecular outcomes.

218 In contrast to the complete absence of Lys⁺ prototrophs in *yku70Δ*, *dnl4Δ* and *mre11Δ*
219 backgrounds, there was only a 10-fold reduction in Lys⁺ frequency when *POL4* was deleted
220 (Figure 2A), which is consistent with most, but not all, repair of HO-generated 3' overhangs
221 requiring Pol4 (LEE AND LEE 2007; TSENG *et al.* 2008). A similar Pol4 dependence of NHEJ was
222 observed using plasmids with defined 3' overhangs but, in contrast to the ZFN ends generated
223 here in a chromosomal context, there was little or no Pol4 dependence with 5' overhangs
224 (DALEY *et al.* 2005a). Of the three major classes of Lys⁺ events observed following ZFN
225 cleavage, only the 2A>3A event (121/183 revertants analyzed) persisted; there were no +CGAA
226 or 1T>2T events detected (Figure 2B). A feature of the 2A>3A event that distinguishes it from
227 the 1T>2T and +CGAA events is that it can occur through the annealing of 5' tails, suggesting
228 that Pol4 may be somewhat less important for gap-filling than for end-filling reactions. Of
229 particular note, the 29-bp deletion event that was rare in WT (~2%; 4/226) accounted for 26%
230 (48/183) of ZFN-initiated events in the *pol4Δ* background. When converted to frequencies, Pol4
231 loss reduced the 2A>3A frequency 5-fold but had no effect on the 29-bp deletion. Finally, the
232 relative importance of Pol4 presence versus its polymerase activity during NHEJ was examined
233 using the *pol4-D367E* allele, which encodes a catalytically inactive protein (WILSON AND LIEBER
234 1999). While the Lys⁺ spectrum in the *pol4-D367E* background was identical to that in the *pol4Δ*
235 mutant, the frequency of Lys⁺ revertants was 2-fold higher than in the *pol4Δ* strain. This
236 suggests a minor structural role for Pol4 not previously detected (WILSON AND LIEBER 1999),
237 which could reflect the stimulation of Dnl4-mediated ligation by Pol4 reported *in vitro* (TSENG
238 AND TOMKINSON 2002).

239

240 **Effects of additional proteins on NHEJ-mediated repair of a ZFN-initiated break**

241 The persistence of Lys⁺ colonies in the *pol4Δ* mutant indicates involvement of other DNA
242 polymerases during repair of 5' overhangs. The Pol ε replicative polymerase has been

243 implicated, for example, in tail removal following the annealing of 3' overhangs (TSENG *et al.*
244 2008). In the current study we focused on roles of the translesion synthesis (TLS) polymerases
245 Pol ζ and Pol η ; *REV3* encodes the catalytic subunit of Pol ζ while the single subunit Pol η
246 protein is encoded by *RAD30*. As observed following cleavage that generates 3' overhangs (LEE
247 AND LEE 2007), there was no significant change in the Lys⁺ frequency in the *rev3 Δ* or *rad30 Δ*
248 single mutant. There was, however, a significant change in the proportional distribution of NHEJ
249 events in each mutant (Figure 3). In the *rev3 Δ* spectrum the proportion of +CGAA events
250 increased 2-fold and accounted for 62% of events (58/94); the proportional decrease in 1T>2T
251 events was significant (12/94) while that of 2A>3A events was not (14/94).

252 Rev3 associates with chromatin near an HO-generated DSB (HIRANO AND SUGIMOTO
253 2006) and we used the *rev3-D975A* allele (JOHNSON *et al.* 2012) to determine whether the
254 alteration in the NHEJ outcomes in the *rev3 Δ* background reflects the presence of the protein or
255 requires its catalytic activity. Both the frequency and spectrum of Lys⁺ colonies in the *rev3-*
256 *D975A* catalytic mutant (JOHNSON *et al.* 2012) were indistinguishable from those of the WT
257 parent, indicating that it is the presence of Rev3 that affects NHEJ outcomes. Rev7 interacts
258 with Rev3 as part of the Pol ζ holoenzyme and we also examined its role in NHEJ. The effect of
259 *REV7* deletion was distinct from that of *REV3* loss. Whereas the spectrum but not the frequency
260 of Lys⁺ revertants was altered in the *rev3 Δ* background, there was a slight reduction in
261 frequency but the spectrum was unchanged in the *rev7 Δ* mutant. The human equivalent of Rev7
262 (*REV7*, also known as *MAD2L2*) restrains end resection to limit HR and promote NHEJ (XU *et*
263 *al.* 2015). Although a similar role for the yeast Rev7 has not been reported, the reduced NHEJ
264 frequency in the *rev7 Δ* background is suggestive of more robust resection in its absence.

265 In the *rad30 Δ* background, the frequency of Lys⁺ revertants was not altered but there
266 again was a significant change in the spectrum of NHEJ events ($p=0.019$). As in the *rev3 Δ*
267 background, the proportion of +CGAA events was elevated (45/94; $p=0.0047$); the proportion of

268 the 2A>3A or 1T>2T events was not significantly altered ($p>0.0125$). Whereas individual
269 deletion of *REV3* or *RAD30* affected the spectrum but not the frequency of Lys⁺ revertants,
270 simultaneous deletion of both was associated with a 2-fold reduction in Lys⁺ frequency as well
271 as a change in the NHEJ spectrum ($p=0.0027$). Instead of the proportional *increase* in +CGAA
272 events observed in the single mutants, there was a specific *decrease* of this specific class in the
273 *rev3Δ rad30Δ* double mutant. While the explanation for this is not obvious, especially given the
274 *POL4* dependence of the +CGAA event, it underscores the complexity of interactions that take
275 place during the error-prone repair of broken ends.

276 NHEJ-mediated repair in *rad52Δ* and *sgs1Δ exo1Δ* backgrounds was examined while
277 measuring potential effects on MMEJ events in surviving colonies. The Rad52 protein is
278 essential for homologous recombination and previous studies have reported either no (FRANK-
279 VAILLANT AND MARCAND 2002; VILLARREAL *et al.* 2012) or very small changes (DENG *et al.* 2014)
280 in NHEJ frequency in a *rad52Δ* background. Sgs1 and Exo1 are redundantly required for the
281 processive resection of 5' ends (MIMITOU AND SYMINGTON 2008) and their loss has no effect on
282 NHEJ (VILLARREAL *et al.* 2012; DENG *et al.* 2014). While we similarly detected no significant
283 change in the Lys⁺ frequency in either a *rad52Δ* or *sgs1Δ exo1Δ* background, the distribution of
284 revertant types was altered in each (Figure 3). Particularly striking was the elevation in “other”
285 NHEJ events: from 16% (37/226) in WT to 44% (41/94) in the *rad52Δ* and to 55% (52/94) in the
286 *sgs1Δ exo1Δ* strain. In both backgrounds, this change reflected a significant increase in the
287 Pol4-independent 29-bp deletion. A distinguishing feature of this specific NHEJ event is that it
288 presumably requires at least some resection to expose complementary repeats, although it is
289 limited by the processive resection of Sgs1/Exo1. If processive resection occurs normally, the
290 data suggest that the 29-bp deletion may remain an option only if recombination cannot be
291 initiated (*rad52Δ* background).

292 Yeast tyrosyl DNA phosphodiesterase (Tdp1) resolves the 5'- and 3'-phosphotyrosyl
293 linkages associated with stabilized topoisomerases (POULIOT *et al.* 1999; NITISS *et al.* 2006) and
294 has a 3' nucleosidase activity that generates 3'-phosphate termini (INTERTHAL *et al.* 2005).
295 Consistent with the latter activity, deletion of *TDP1* was associated with an increase in the
296 complete fill-in of 5' overhangs in a plasmid-based NHEJ assay (BAHMED *et al.* 2010). A similar
297 effect was not observed, however, when repair of a ZFN-generated chromosomal break was
298 examined by deep sequencing (LIANG *et al.* 2016). In our system *TDP1* deletion had no effect
299 on the frequency of Lys⁺ revertants but did alter the spectrum of events (p=0.013). Among the
300 three major classes of events there was a significant change only in the proportion of +CGAA
301 events, (from 69/226 in WT to 53/112 in *tdp1Δ*; p=0.0055). This is consistent with a subtle effect
302 on Tdp1 on the ability to fill 5' overhangs.

303

304 **Genetic control of the Pol4-independent 29-bp deletion**

305 The model for the 29-bp deletion, which accounted for half of revertants in the *pol4Δ*
306 background, requires 5'>3' resection to expose GCC repeats that flank the ZFN cleavage site,
307 annealing between complementary strands of GCC repeats, and cleavage of single-strand 3'
308 tails to allow filling of flanking gaps (Figure 1C). We first examined whether TLS polymerases
309 are relevant to the Pol4-independent filling of the small gaps flanking the annealed segment.
310 *REV3*, *RAD30* or both were deleted from the *pol4Δ* background and there were changes in the
311 frequency and/or spectra of Lys⁺ revertants in each relative to the *pol4Δ* single mutant (Figure
312 4). The Lys⁺ frequency increased 2.0- and 3.7-fold, respectively, in the *pol4Δ rad30Δ* and *pol4Δ*
313 *rev3Δ* backgrounds but was not significantly altered in the *pol4Δ rev3Δ rad30Δ* triple mutant.
314 The proportion of the 29-bp deletion was reduced in the *pol4Δ rev3Δ* and *pol4Δ rev3Δ rad30Δ*
315 backgrounds but was unaffected in the *pol4Δ rad30Δ* mutant. The frequencies of the 29-bp
316 deletion were estimated by multiplying Lys⁺ frequencies and corresponding proportions of the

317 29-bp deletion. The 29-bp deletion frequency was unaffected by deletion of *REV3* or *RAD30*
318 individually in the *pol4Δ* background but was reduced 10-fold in the *pol4Δ rev3Δ rad30Δ* triple
319 mutant. These data demonstrate that Pol ζ and Pol η have redundant roles during the Pol4-
320 independent gap filling required to generate the 29-bp deletion.

321 Although sporadic deletions involving other short repeats were observed among
322 revertants in all genetic backgrounds (Table S2), the GCC repeats at the endpoint of the 29-bp
323 deletion were notable because they are close to and symmetrically flank the ZFN cleavage site.
324 Furthermore, the frequency of the 29-bp deletion was elevated when the long-range resection
325 pathways were eliminated (*exo1Δ sgs1Δ* double mutant; Figure 3). Given the repressive effect
326 of resection on this event and the symmetry/proximity of the GCC repeats to the ZFN cleavage
327 site, we considered the possibility that Mre11 nuclease activity might be required to expose the
328 repeats within short 3' overhangs. Mre11 nicks the 5' strand 30-35 nt from a Ku-bound end and
329 expansion of the nick into a gap by its 3'→5' exonuclease activity degrades the 5' end to
330 displace Ku and create a short 3' tail (reviewed in REGINATO AND CEJKA 2020). To examine the
331 relevance Mre11 nuclease activity to the NHEJ-dependent 29-bp deletion, the nuclease-dead
332 *mre11-D56N* allele (LLORENTE AND SYMINGTON 2004) was introduced into the *pol4Δ*
333 background. The Lys⁺ frequency increased 12-fold in the double mutant relative to the *pol4Δ*
334 single mutant and this was accompanied by a change in the distribution of revertant types
335 (Figure 4). Almost all revertants had the 2A>3A event (91/96; p<0.0001) and only a single 29-bp
336 deletion was observed. The *mre11-D56N* allele thus had a strong stimulatory effect on the
337 frequency 2A>3A event, but its effect on the frequency of the 29-bp deletion was unclear.

338 To preclude occurrence of the 2A>3A event and allow more specific focus on the 29-bp
339 deletion in the *pol4Δ* background, we changed the spacer sequence of the ZFN cleavage site
340 from ACGAAT to ACGTAT. With the new ACGTAT spacer in the *POL4* background, there were
341 similar numbers of +CGTA and 1T>2T events (43/116 and 63/116, respectively), as there were

342 with the original spacer, and the 29-bp deletion remained rare (2/116). Given the absence of +4
343 and 1T>2T events with the original ACGAAT spacer in the *pol4Δ* background, we assumed that
344 the 29-bp deletion would be present in almost all Lys⁺ colonies derived using the new ACGTAT
345 spacer. In the *pol4Δ* background with the new spacer, however, half of revertants contained the
346 +CGTA event (54/37) and 30% had the 29-bp deletion (37/118); there still were no 1T>2T
347 events. In the absence of Pol4, the data suggest that the end-annealing that generates the
348 2A>3A event may precede complete filling and obscure its occurrence.

349 Elimination of Mre11 nuclease activity in a *POL4* background with the new spacer
350 increased the frequency of Lys⁺ revertants 14-fold and altered the proportions of +CGTA and
351 1T>2T events (Tables S1 and S2). This mirrors the differential effects of the *mre11-D56N* allele
352 on the NHEJ spectrum observed with the original ACGAAT spacer. Introduction of the *mre11-*
353 *D56N* allele into the *pol4Δ* background resulted in a 9-fold increase in Lys⁺ frequency relative to
354 the *pol4Δ* single mutant, which was similar to the increase observed with the original spacer. In
355 contrast to the large proportional decrease in the 29-bp deletion in the *pol4Δ mre11-D56N*
356 background with original spacer, however, there was no reduction with the new spacer. This
357 demonstrates that Mre11 nuclease activity is not required to expose the GCC repeats at the
358 endpoints of the 29-bp deletion.

359 In the model depicted in Figure 1C end resection allows annealing between
360 complementary strands of the GCC repeat, thereby creating 3' tails that must be removed prior
361 to gap filling and ligation. The Rad1-Rad10 nuclease is required for the removal of long 3' tails
362 during SSA, but tails <30 nt are efficiently removed by the exonuclease activity of Pol δ (PAQUES
363 AND HABER 1997). In the *pol4Δ* strain containing the new spacer sequence, elimination of the
364 exonuclease activity of Pol δ (*pol3-DV* allele; (JIN *et al.* 2001) reduced the Lys⁺ frequency 2.5-
365 fold and this reflected the complete absence of the 29-bp deletion among revertants (0/95

366 revertants; $p < 0.0001$; Figure 4). These data demonstrate that the exonuclease activity of Pol δ
367 is required during creation of the 29-bp deletion.

368 The data presented above present a conundrum with respect to the genetic control of
369 the NHEJ-dependent 29-bp deletion. It was antagonized by processive nuclease activity (*sgs1 Δ*
370 *exo1 Δ* background) and yet did not appear to depend on the nuclease activity of Mre11 (*pol4 Δ*
371 *mre11-D56N* background). How then are the complementary strands of the GCC direct repeats
372 exposed? One possibility is that the DNA melting activity of the MRX complex is responsible.
373 This requires the ATPase activity of Rad50 (CANNON *et al.* 2013), which also is required for
374 NHEJ in yeast (ZHANG AND PAULL 2005). The strong dependence of the 29-bp deletion on the
375 exonuclease activity of Pol δ (*pol4 Δ pol3-DV* mutant) suggests an alternative possibility in which
376 it is the degradation of the recessed 3' ends by Pol δ that exposes the GCC repeats. Regardless
377 of how the complementary strands of the GCC repeats are exposed, the Ku dependence of the
378 29-bp deletion suggests either that Ku remains associated with the ends or that Ku re-engages
379 the ends after displacement. Ku interacts with duplexes with 30-nt tails almost as well as with
380 fully duplex DNA *in vitro* (FALZON *et al.* 1993); longer, 60-nt tails are not efficiently bound by Ku
381 (FOSTER *et al.* 2011).

382

383 **Survivors of continuous ZFN expression**

384 Selection for colonies on rich medium containing galactose provides an unbiased
385 analysis of end-joining events that confer resistance to continuous ZFN expression. As reported
386 previously, only half of survivors (83/155) in the WT background lost the enzyme cleavage site
387 (SHALTZ AND JINKS-ROBERTSON 2021) and these were of two major types: a Ku-dependent +AC
388 event that expanded two copies an AC dinucleotide spanning the 6-bp ZFN spacer (36/83) and
389 Ku-independent large deletions that removed the cleavage site (47/83). The +AC event was not
390 detectable in the reversion assay, which selects net +1 events, and was hypothesized to arise

391 by misincorporation-slippage during proximal end filling (Figure 1B). The rarity of net +1 events
392 in the survivor assay indicates that they are minor events relative to +AC. The large deletions
393 were either 1.2 kb (36/47) or 11.7 kb (11/47) in size (Figure 5A) and because the deletion
394 junctions were in 13- or 14-bp direct repeats, respectively, we concluded that these were MMEJ
395 events. In the current analyses, the frequencies and profiles of survivors were examined in the
396 genetic backgrounds described above for Lys⁺ revertants. Only those mutants that were
397 different from the WT strain in terms of the frequency and/or spectrum of site-loss survivors are
398 discussed (see Tables S1 and S3 for all data).

399 Because NHEJ and MMEJ proportions are similar among survivors, the complete loss of
400 either pathway would be expected to reduce the survival frequency only 2-fold. Indeed, as
401 reported previously in the *yku70*Δ background (SHALTZ AND JINKS-ROBERTSON 2021), the
402 survival frequency was reduced 2-fold in the NHEJ-deficient *pol4*Δ (Figure 5B-C) and *dnl4*Δ
403 (Tables S1 and S3) backgrounds and only large deletions were detected. Although NHEJ
404 events were also absent in an *mre11*Δ strain, there was 5.9-fold reduction in overall survival
405 frequency rather than the expected 2-fold (Figure 5B). Survivor frequencies were also low in
406 *rad52*Δ single and *sgs1*Δ *exo1*Δ double-mutant backgrounds, with reductions of 6.7- and 16.7-
407 fold, respectively, relative to WT. Impaired growth was a common feature of these three mutant
408 backgrounds, and we suggest that this may be responsible for the large decrease in survivor
409 frequency. We favor this interpretation because, in contrast to the survivor assay, the NHEJ
410 frequency as measured by Lys⁺ reversion was not affected in either the *rad52*Δ or *sgs1*Δ *exo1*Δ
411 background (Figure 3). It is possible that repetitive cleavage by a ZFN impairs viability more
412 when cells can continue to divide (nonselective rich medium) than when cells are plated under
413 conditions where error-prone repair must restore prototrophy before cells can begin dividing.

414 In addition to reduced survival, the spectrum of events among survivors was altered in
415 the *rad52*Δ and *sgs1*Δ *exo1*Δ backgrounds relative to WT (p=0.0013 and p<0.0001,

416 respectively). There was a reduction in the proportion of large deletions in the *rad52* Δ mutant,
417 (from 47/83 to 19/58; $p=0.009$), suggestive of a partial requirement of Rad52 for the MMEJ-
418 mediated large deletions. In an earlier study that systematically examined the effect of repeat
419 size on microhomology-mediated end joining (VILLARREAL *et al.* 2012), Rad52 promoted end
420 joining for repeats 15 bp or larger, suggesting a variation of SSA as the mechanism, and
421 strongly inhibited end-joining between repeats 12 bp or smaller. The sizes of the repeats at the
422 MMEJ endpoints in the current study (13-14 bp) are in the transition zone for Rad52
423 dependence. In the *sgs1* Δ *exo1* Δ double mutant the proportion of large deletions was reduced
424 10-fold: from 47/83 in WT to only 2/39. This reduction likely reflects the extensive resection
425 required to expose the junction repeats of large deletions and is consistent with results obtained
426 with similar large deletions (VILLARREAL *et al.* 2012). This is in contrast to the suppressive effect
427 of Sgs1/Exo1 resection (as well as Mre11 presence) with respect to Ku-independent deletions
428 between 12-bp repeats very close to I-SceI-generated ends (DENG *et al.* 2014). The resection-
429 related suppression is similar to that described above for the Pol4-independent 29-bp deletion,
430 although the 29-bp deletion is Ku- and Mre11-dependent (see above).

431 Because the nuclease activity of Mre11 inhibits NHEJ, an elevation in the NHEJ-
432 dependent +AC event was expected in an *mre11-D56N* background. There, however, was
433 neither a change in survivor frequency nor spectrum relative to WT. This result provides further
434 support for an influence of Mre11 nuclease activity on specific NHEJ outcomes, as inferred from
435 the variable effect of the *mre11-D56N* allele on Lys⁺ revertant types in the WT and *pol4* Δ
436 backgrounds. Finally, there was 2.7-fold increase in survivor frequency in a *rev7* Δ background
437 that specifically reflected an increase in MMEJ; no effect on frequency or spectra was observed
438 upon loss of *REV3* (Table S1). These data more strongly support a potentially suppressive role
439 of Rev7 on processive resection in yeast, as inferred previously from the slightly increased
440 frequency of Lys⁺ revertants.

441 The Rad1-Rad10 endonuclease is required to remove 3' tails during SSA (IVANOV AND
442 HABER 1995) and a similar importance for Rad1 in MMEJ was inferred through analysis of HO-
443 initiated 2-kb deletions between 18-bp direct repeats (VILLARREAL *et al.* 2012). The strong
444 Rad52 dependence for deletions between 18-bp, however, suggests that the events were a
445 variation of SSA. We thus re-examined the requirement for Rad1 for the large, NHEJ-
446 independent deletions in our system. With the smaller (13- and 14-bp) repeats, there was no
447 significant change in either the frequency or the distribution of survivor types in a *rad1Δ*
448 background (Figure 5; see Tables S1-S3 for similar *rad10Δ* data). To potentially identify the
449 relevant structure-specific nuclease that removes 3' tails during MMEJ, we examined survival in
450 *mus81Δ* single and *rad1Δ mus81Δ* double mutants, as well as in an *slx4Δ* background. Mus81
451 can process 3' flaps (SCHWARTZ AND HEYER 2011) while Slx4 is a scaffold for multiple structure-
452 specific endonucleases (CUSSIOL *et al.* 2017). There was no proportional decrease in large
453 deletions in any of these additional mutant backgrounds (Table S3). Either a different nuclease
454 is relevant, or there is functional redundancy between the nucleases examined. Just as there is
455 a size-related transition in Rad52 dependence for microhomology-mediated deletions
456 (VILLARREAL *et al.* 2012), there may be a similar transition in terms of a requirement for Rad1-
457 Rad10 in 3'-tail removal. One interesting possibility is that Rad52-driven annealing dictates
458 whether subsequent tail removal is dependent on Rad1-Rad10.

459

460 **The physiological state of cells affects repair of ZFN-induced DSBs**

461 NHEJ-mediated ligation of a linearized plasmid is more efficient when non-growing (NG)
462 cells are transformed than when growing cells are transformed (KARATHANASIS AND WILSON
463 2002). To examine the effects of growth state on error-prone repair of a chromosomal DSB,
464 either non-growing (NG) or isolated G0 cells were plated in the presence of galactose. The Lys⁺
465 frequency in NG cells was 2.4-fold higher than in growing cells and there were proportionally

466 fewer +CGAA events among revertants (Figure 6A). When the event types were converted to
467 frequencies, however, the +CGAA frequency was unaltered while the frequencies of 2A>3A,
468 1T>2T and other NHEJ events were each elevated about 3-fold. There was a further stimulation
469 of the Lys⁺ frequency when G0 cells were plated: 6.8- and 2.8-fold relative to growing and NG
470 cells, respectively. Interestingly, there was a very large proportional increase in the +CGAA
471 class of events in G0 cells that corresponded to a 10-fold increase in its frequency relative to
472 growing/NG cells; the frequencies of the other classes changed little relative to NG cells.

473 In terms of surviving colonies that had lost the ZFN cleavage site, the overall frequency
474 also was elevated relative to growing cells: 2.4-fold in NG cells and 5.4-fold in G0 cells (Figure
475 6B). The spectrum of survivors was also altered. As expected of events that require extensive
476 resection, the proportion of large deletions was greatly reduced: from 0.56 (47/83) in growing
477 cells to 0.16 (15/92) and 0.05 (4/79) when NG and G0 cells, respectively, were plated. Given the
478 large increase in survival, however, the large-deletion frequency was reduced only about 2-fold
479 in NG and G0 cells. In terms of frequency, the +AC event was elevated 4.7-fold in NG cells and
480 8.7-fold in G0 cells; the frequency of “other” events was similarly elevated. The data
481 demonstrate that NHEJ-mediated repair of a ZFN-generated DSB is more efficient in NG/G0
482 cells than in growing cells, and that physiological state additionally affects how the resulting
483 ends are modified during error-prone repair.

484

485 **CONCLUSIONS**

- 486 • Following ZFN cleavage, half of error-prone repair events reflected small insertions/deletions
487 at the cleavage site (NHEJ) and half were large deletions (MMEJ).
- 488 • In contrast to the complete dependence of NHEJ on Ku, Mre11 and Dnl4, loss of Pol4
489 reduced NHEJ only 10-fold. Although most NHEJ events were dependent on Pol4, a
490 recurrent 29-bp deletion was Pol4-independent. This deletion was suppressed by

- 491 processive 5' end resection and required the 3'>5' exonuclease activity of the replicative
492 DNA polymerase δ .
- 493 • Mre11 nuclease activity suppressed NHEJ and additionally affected the spectrum of events
494 but had no effect on MMEJ.
 - 495 • Pol ζ and Pol η altered NHEJ outcomes in both the presence and absence of Pol4.
 - 496 • Absence of the Rev3 or Rev7 component of Pol ζ had different effects on DSB repair. Of
497 particular note, the suppressive effect of Rev7 on MMEJ is consistent with a modulation of
498 resection.
 - 499 • Long single-strand tails created by resection must be removed to complete MMEJ, but
500 neither Rad1, Mus81 nor Sxl4 was required for this step.
 - 501 • NHEJ was increased and MMEJ was decreased when ZFN cleavage occurred in non-
502 dividing cells.

503

504 **ACKNOWLEDGEMENTS**

505 This work was supported by National Institutes of Health grant R35GM118077 to SJR.

506

507 **REFERENCES**

- 508 Bahmed, K., K. C. Nitiss and J. L. Nitiss, 2010 Yeast Tdp1 regulates the fidelity of
509 nonhomologous end joining. *Proc. Natl. Acad. Sci. USA* 107: 4057-4062.
- 510 Beumer, K., G. Bhattacharyya, M. Bibikova, J. K. Trautman and D. Carroll, 2006 Efficient gene
511 targeting in *Drosophila* with zinc-finger nucleases. *Genetics* 172: 2391-1403.
- 512 Cannon, B., J. Kuhnlein, S. H. Yang, A. Cheng, D. Schindler *et al.*, 2013 Visualization of local
513 DNA unwinding by Mre11/Rad50/Nbs1 using single-molecule FRET. *Proc. Natl. Acad. Sci. USA* 110: 18868-18873.
- 514
- 515 Cho, J. E., and S. Jinks-Robertson, 2019 Deletions associated with stabilization of the Top1
516 cleavage complex in yeast are products of the nonhomologous end-joining pathway.
517 *Proc. Natl. Acad. Sci. USA* 116: 22683-22691.
- 518 Cussiol, J. R., D. Dibitetto, A. Pelliccioli and M. B. Smolka, 2017 Slx4 scaffolding in homologous
519 recombination and checkpoint control: lessons from yeast. *Chromosoma* 126: 45-58.
- 520 Daley, J. M., R. L. Laan, A. Suresh and T. E. Wilson, 2005a DNA joint dependence of pol X
521 family polymerase action in nonhomologous end joining. *J. Biol. Chem.* 280: 29030-
522 29037.

- 523 Daley, J. M., P. L. Palmbo, D. Wu and T. E. Wilson, 2005b Nonhomologous end joining in
524 yeast. *Annu. Rev. Genet.* 39: 431-451.
- 525 Deng, S. K., B. Gibb, M. J. de Almeida, E. C. Greene and L. S. Symington, 2014 RPA
526 antagonizes microhomology-mediated repair of DNA double-strand breaks. *Nat. Struct.*
527 *Mol. Biol.* 21: 405-412.
- 528 Falzon, M., J. W. Fewell and E. L. Kuff, 1993 EBP-80, a transcription factor closely resembling
529 the human autoantigen Ku, recognizes single- to double-strand transitions in DNA. *J.*
530 *Biol. Chem.* 268: 10546-10552.
- 531 Foster, S. S., A. Balestrini and J. H. Petrini, 2011 Functional interplay of the Mre11 nuclease
532 and Ku in the response to replication-associated DNA damage. *Mol Cell Biol* 31: 4379-
533 4389.
- 534 Frank-Vaillant, M., and S. Marcand, 2002 Transient stability of DNA ends allows
535 nonhomologous end joining to precede homologous recombination. *Mol. Cell* 10: 1189-
536 1199.
- 537 Goldstein, A. L., and J. H. McCusker, 1999 Three new dominant drug resistance cassettes for
538 gene disruption in *Saccharomyces cerevisiae*. *Yeast* 15: 1541-1553.
- 539 Haber, J. E., 2012 Mating-type genes and *MAT* switching in *Saccharomyces cerevisiae*.
540 *Genetics* 191: 33-64.
- 541 Hatkevich, T., D. E. Miller, C. A. Turcotte, M. C. Miller and J. Sekelsky, 2021 A pathway for
542 error-free non-homologous end joining of resected meiotic double-strand breaks. *Nucleic*
543 *Acids Res.* 49: 879-890.
- 544 Hirano, Y., and K. Sugimoto, 2006 ATR homolog Mec1 controls association of DNA polymerase
545 ζ -Rev1 complex with regions near a double-strand break. *Curr. Biol.* 16: 586-590.
- 546 Interthal, H., H. J. Chen and J. J. Champoux, 2005 Human Tdp1 cleaves a broad spectrum of
547 substrates, including phosphoamide linkages. *J. Biol. Chem.* 280: 36518-36528.
- 548 Ivanov, E. L., and J. E. Haber, 1995 *RAD1* and *RAD10*, but not other excision repair genes, are
549 required for double-strand break-induced recombination in *Saccharomyces cerevisiae*.
550 *Mol. Cell. Biol.* 15: 2245-2251.
- 551 Ivanov, E. L., N. Sugawara, J. Fishman-Lobell and J. E. Haber, 1996 Genetic requirements for
552 the single-strand annealing pathway of double-strand break repair in *Saccharomyces*
553 *cerevisiae*. *Genetics* 142: 693-704.
- 554 Jin, Y. H., R. Obert, P. M. Burgers, T. A. Kunkel, M. A. Resnick *et al.*, 2001 The 3'→5'
555 exonuclease of DNA polymerase δ can substitute for the 5' flap endonuclease
556 Rad27/Fen1 in processing Okazaki fragments and preventing genome instability. *Proc.*
557 *Natl. Acad. Sci. USA* 98: 5122-5127.
- 558 Johnson, R. E., L. Prakash and S. Prakash, 2012 Pol31 and Pol32 subunits of yeast DNA
559 polymerase δ are also essential subunits of DNA polymerase ζ . *Proc. Natl. Acad. Sci.*
560 *USA* 109: 12455-12460.
- 561 Jung, D., C. Giallourakis, R. Mostoslavsky and F. W. Alt, 2006 Mechanism and control of V(D)J
562 recombination at the immunoglobulin heavy chain locus. *Annu. Rev. Immunol.* 24: 541-
563 570.
- 564 Karathanasis, E., and T. E. Wilson, 2002 Enhancement of *Saccharomyces cerevisiae* end-
565 joining efficiency by cell growth stage but not by impairment of recombination. *Genetics*
566 161: 1015-1027.
- 567 Keeney, S., 2008 Spo11 and the formation of DNA double-strand breaks in meiosis. *Genome*
568 *Dyn. Stab.* 2: 81-123.
- 569 Kozmin, S. G., and S. Jinks-Robertson, 2013 The mechanism of nucleotide excision repair-
570 mediated UV-induced mutagenesis in nonproliferating cells. *Genetics* 193: 803-817.
- 571 Lee, K., and S. E. Lee, 2007 *Saccharomyces cerevisiae* Sae2- and Tel1-dependent single-
572 strand DNA formation at DNA break promotes microhomology-mediated end joining.
573 *Genetics* 176: 2003-2014.

- 574 Lemos, B. R., A. C. Kaplan, J. E. Bae, A. E. Ferrazzoli, J. Kuo *et al.*, 2018 CRISPR/Cas9
575 cleavages in budding yeast reveal templated insertions and strand-specific
576 insertion/deletion profiles. *Proc. Natl. Acad. Sci. USA* 115: E2040-e2047.
- 577 Liang, Z., S. Sunder, S. Nallasivam and T. E. Wilson, 2016 Overhang polarity of chromosomal
578 double-strand breaks impacts kinetics and fidelity of yeast non-homologous end joining.
579 *Nucleic Acids Res.* 44: 2769-2781.
- 580 Llorente, B., and L. S. Symington, 2004 The Mre11 nuclease is not required for 5' to 3' resection
581 at multiple HO-induced double-strand breaks. *Mol. Cell. Biol.* 24: 9682-9694.
- 582 Ma, J. L., E. M. Kim, J. E. Haber and S. E. Lee, 2003 Yeast Mre11 and Rad1 proteins define a
583 Ku-independent mechanism to repair double-strand breaks lacking overlapping end
584 sequences. *Mol. Cell. Biol.* 23: 8820-8828.
- 585 Mimitou, E. P., and L. S. Symington, 2008 Sae2, Exo1 and Sgs1 collaborate in DNA double-
586 strand break processing. *Nature* 455: 770-774.
- 587 Moore, A., M. Dominska, P. Greenwell, A. Y. Aksenova, S. Mirkin *et al.*, 2018 Genetic control of
588 genomic alterations induced in yeast by interstitial telomeric sequences. *Genetics* 209:
589 425-438.
- 590 Moreau, S., J. R. Ferguson and L. S. Symington, 1999 The nuclease activity of Mre11 is
591 required for meiosis but not for mating type switching, end joining, or telomere
592 maintenance. *Mol. Cell. Biol.* 19: 556-566.
- 593 Nitiss, K. C., M. Malik, X. He, S. W. White and J. L. Nitiss, 2006 Tyrosyl-DNA
594 phosphodiesterase (Tdp1) participates in the repair of Top2-mediated DNA damage.
595 *Proc. Natl. Acad. Sci. U.S.A.* 103: 8953-8958.
- 596 Paques, F., and J. E. Haber, 1997 Two pathways for removal of nonhomologous DNA ends
597 during double-strand break repair in *Saccharomyces cerevisiae*. *Mol. Cell. Biol.* 17:
598 6765-6771.
- 599 Pouliot, J. J., K. C. Yao, C. A. Robertson and H. A. Nash, 1999 Yeast gene for a Tyr-DNA
600 phosphodiesterase that repairs topoisomerase I complexes. *Science* 286: 552-555.
- 601 Reginato, G., and P. Cejka, 2020 The MRE11 complex: A versatile toolkit for the repair of
602 broken DNA. *DNA Repair* 91-92: 102869.
- 603 Schwartz, E. K., and W. D. Heyer, 2011 Processing of joint molecule intermediates by structure-
604 selective endonucleases during homologous recombination in eukaryotes. *Chromosoma*
605 120: 109-127.
- 606 Sfeir, A., and L. S. Symington, 2015 Microhomology-Mediated End Joining: A Back-up Survival
607 Mechanism or Dedicated Pathway? *Trends Biochem Sci* 40: 701-714.
- 608 Shaltz, S., and S. Jinks-Robertson, 2021 Mutagenic repair of a ZFN-induced double-strand
609 break in yeast: Effects of cleavage site sequence and spacer size. *DNA Repair* 108:
610 103228.
- 611 Storici, F., and M. A. Resnick, 2006 The *delitto perfetto* approach to *in vivo* site-directed
612 mutagenesis and chromosome rearrangements with synthetic oligonucleotides in yeast.
613 *Methods Enzymol.* 409: 329-345.
- 614 Symington, L. S., 2016 Mechanism and regulation of DNA end resection in eukaryotes. *Crit.*
615 *Rev. Biochem. Mol. Biol.* 51: 195-212.
- 616 Symington, L. S., R. Rothstein and M. Lisby, 2014 Mechanisms and regulation of mitotic
617 recombination in *Saccharomyces cerevisiae*. *Genetics* 198: 795-835.
- 618 Teo, S. H., and S. P. Jackson, 1997 Identification of *Saccharomyces cerevisiae* DNA ligase IV:
619 involvement in DNA double-strand break repair. *EMBO J.* 16: 4788-4795.
- 620 Tseng, H. M., and A. E. Tomkinson, 2002 A physical and functional interaction between yeast
621 Pol4 and Dnl4-Lif1 links DNA synthesis and ligation in nonhomologous end joining. *J.*
622 *Biol. Chem.* 277: 45630-45637.

- 623 Tseng, S. F., A. Gabriel and S. C. Teng, 2008 Proofreading activity of DNA polymerase Pol2
624 mediates 3'-end processing during nonhomologous end joining in yeast. PLoS Genet. 4:
625 e1000060.
- 626 Villarreal, D. D., K. Lee, A. Deem, E. Y. Shim, A. Malkova *et al.*, 2012 Microhomology directs
627 diverse DNA break repair pathways and chromosomal translocations. PLoS Genet. 8:
628 e1003026.
- 629 Wilson, T. E., and M. R. Lieber, 1999 Efficient processing of DNA ends during yeast
630 nonhomologous end joining. Evidence for a DNA polymerase beta (Pol4)-dependent
631 pathway. J. Biol. Chem. 274: 23599-23609.
- 632 Xu, G., J. R. Chapman, I. Brandsma, J. Yuan, M. Mistrik *et al.*, 2015 REV7 counteracts DNA
633 double-strand break resection and affects PARP inhibition. Nature 521: 541-544.
- 634 Zhang, X., and T. T. Paull, 2005 The Mre11/Rad50/Xrs2 complex and non-homologous end-
635 joining of incompatible ends in *S. cerevisiae*. DNA Repair 4: 1281-1294.
- 636

637

638

639 **FIGURE LEGENDS**

640 **Figure 1.** ZFN cleavage of spacer ACGAAT and error-prone repair events. **(A)** The sequence of
641 the 24 bp *rosy* sequence inserted into *LYS2* is shown, with the three bases recognized by each
642 zinc finger (blue or red ovals for RyA and RyB, respectively) indicated. The yellow ovals
643 represent the dimerized *FokI* domains; the 6-bp spacer is in red font and triangles indicate
644 positions of enzyme-generated nicks that create 4-bp 5' overhangs. **(B)** Sequences added
645 during repair events are in lowercase red. Only the first three classes (+CGAA, 2A>3A and
646 1T>2T) generate Lys⁺ revertants; the fourth class (+AC) was only observed only among
647 survivors. Complete filling of ends duplicates the region bounded by the ZFN nicks (+CGAA)
648 while out-of-register pairing between an A and T in the overhangs generates the 2A>3A
649 mutation. Duplication of the T (1T>2T) adjacent to the distal overhang can be generated by
650 misincorporation-realignment, followed by ligation of the re-created 4-nt overhangs. The +AC
651 event can be generated by a similar misincorporation-realignment mechanism during initial
652 filling of the proximal overhang. **(C)** Mechanism for the NHEJ-dependent 29-bp deletion that is
653 frequent among Lys⁺ revertants in the *pol4Δ* background. Resection of the 5' ends allows

654 pairing between GCC repeats (red) that flank the DSB. Subsequent removal of 3' tails and filling
655 of flanking gaps (red lowercase) completes repair.

656

657 **Figure 2.** Frequencies and distributions of Lys⁺ revertants in strains with altered core NHEJ
658 proteins. **(A)** Mean frequencies of Lys⁺ colonies; error bars are 95% confidence intervals for the
659 mean. **(B)** Distributions of the five major NHEJ types among revertants. Overall distributions
660 were compared to WT using a global 2 x 5 contingency chi square test (p values are above
661 each spectrum) and if p<0.05, then individual mutation types were compared using the
662 Bonferroni correction to determine significance (p<0.05/5); asterisks indicate a significant
663 proportional class increase/decrease.

664

665 **Figure 3.** Altered frequencies and distributions of Lys⁺ revertants in mutant backgrounds. Mean
666 frequencies of Lys⁺ colonies are shown; error bars are 95% confidence intervals for the means.
667 The overall distribution of the five major NHEJ types in each mutant background was compared
668 to WT using a 2 x 5 contingency chi square test (ns, not significant). If the global p value (above
669 each spectrum) was less than 0.05, individual mutation classes were compared using the
670 Bonferroni correction to determine significance (p<0.05/5); asterisks indicate a significant
671 proportional increase/decrease.

672

673 **Figure 4.** Genetic control of the Pol4-independent, 29-bp deletion. **(A)** Mean frequencies of Lys⁺
674 colonies; error bars are 95% confidence intervals for the means. **(B)** The overall distribution of
675 the three major NHEJ types in each mutant background. With the ACGAAT spacer only the
676 2A>3A, the 29-bp deletion, and random “other” events were observed; there were no 1T>2T or
677 +CGAA events. Changing the ACGAAT spacer to ACGTAT eliminated the 2A>3A event (orange
678 cross-hatched), which was replaced by +CGTA (blue). Each distribution was compared to the
679 corresponding WT using a 2 x 3 contingency chi square test (ns, not significant). If the global p

680 value (above each spectrum) was less than 0.05, individual mutation classes were compared
681 using the Bonferroni correction to determine significance ($p < 0.05/3$); asterisks indicate a
682 significant proportional increase/decrease.

683

684 **Figure 5.** Genetic control of the survivor frequency and spectrum. **(A)** The two types of
685 recurrent large deletions detected among surviving colonies. The 1.2 kb deletion as endpoints in
686 13-bp direct repeats (CCAAGCTACTACA), one of which overlaps the DNA binding site of the
687 RyB subunit of the ZFN. The 11.7 kb deletion has endpoints in 14-bp direct repeats
688 (TGGAATAAAAAAAAA) and removes the *LYS2*-flanking genes *TKL2* and *RAD16* (not shown).
689 **(B)** Mean frequencies of surviving colonies that lost the ZFN cleavage site; error bars are 95%
690 confidence intervals for the means. **(C)** The distributions of the three major survivor types are
691 shown. Each mutant distribution was compared to the WT using a 2 x 3 contingency chi square
692 test (ns, not significant). If the global p value (above each spectrum) was less than 0.05,
693 individual mutation classes were compared using the Bonferroni correction to determine
694 significance ($p < 0.05/3$); asterisks indicate a significant proportional increase/decrease.

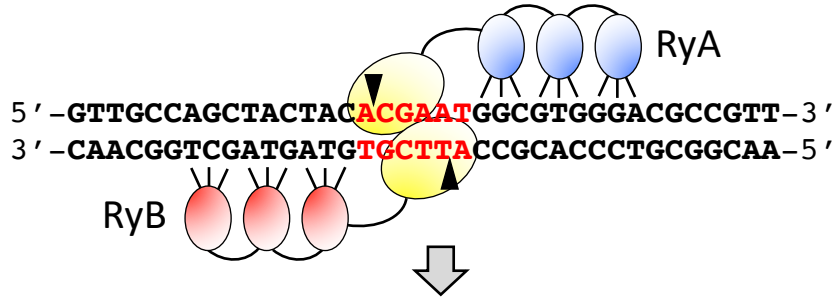
695

696 **Figure 6.** Alterations in error-prone DSB repair in NG and G0 cells. **(A)** Mean *Lys*⁺ frequencies
697 and revertant-type distributions in growing, NG and G0 cells. **(B)** Mean survivor frequencies and
698 event-type distributions in growing, NG and G0 cells. Error bars are 95% CIs for mean
699 frequencies. Event-type distributions were compared to growing cells using a 2x4 or 2x3
700 contingency chi square test for revertants or survivors, respectively; ns, not significant. If the
701 global p value was < 0.05 (above each spectrum), then individual mutation types were compared
702 using the Bonferroni correction to determine significance; asterisks indicate a significant
703 proportional increase/decrease.

704

705

A



5' -GTTGCCAGCTACTACA **CGAAT**TGGCGTGGGACGCCGTT-3'
 3' -CAACCGTCGATGATGT**TGCTT** ACCGCACCCTGCGGCAA-5'

B

ACA**cgaa** **CGAAT**GG → ACA**cgaaCGAAT**GG **+CGAA**
 TGT**TGCTT** gctt**ACC** → TGT**TGCTTgcttA**ACC

ACA ^{CG} **AAT**GG → ACA**cgaa**AATGG **2A>3A**
 TGT**TGCTT** ACC → TGT**TGCTTt**ACC

ACA **CGAAT**GG → AC**ACGAAT**TTGG **1T>2T**
 TGT**TGCTT** a**ACC** → TGT**TGCTTtA**ACC

(AC)
 CT**Aca** **CGAAT**GG → CT**ACa**c**CGAAT**GG **+AC**
 GAT**TGCTT** ACC → GAT**TgtGCTT**AACC

C

TTCAAAGTT**GCC**AGCTACTACA → **CGAAT**TGGCGTGGGAC**GCC**GTTTGGCCT-3'
 3' -AAGTTTCA**CGG**TCGATGATGT**GCTT** ACCGCACCCTG**CGG**CAAACCGGA

AGCTACTACA-3'
 TTCAAAGTT**GCC** GGCCT
 AAGTT **CGG**GAAACCGGA
 3' -ACCGCACCCTG

TTCAAAGTT**GCC**gtttGGCCT
 AAGTT**tcaaCGG**CAAACCGGA **29-bp deletion**

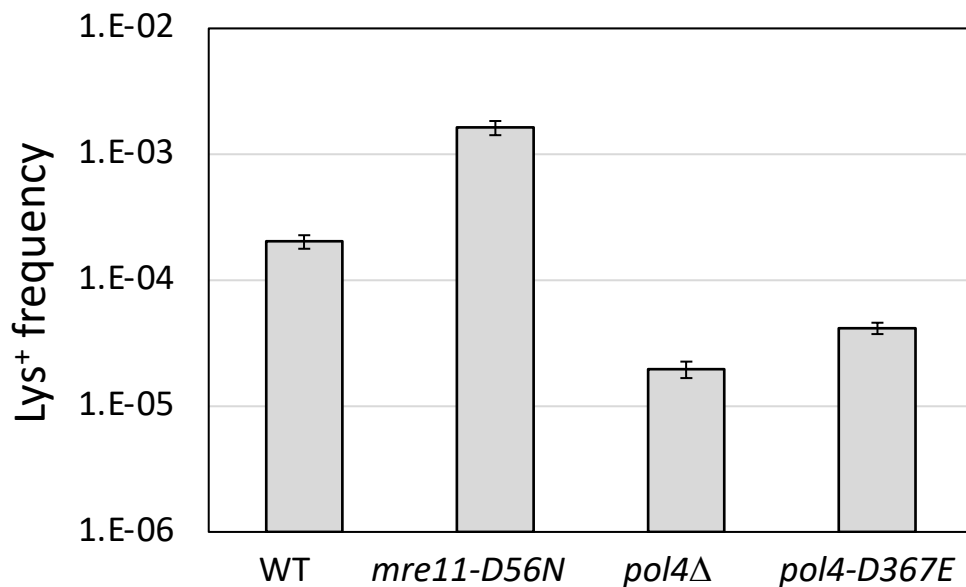
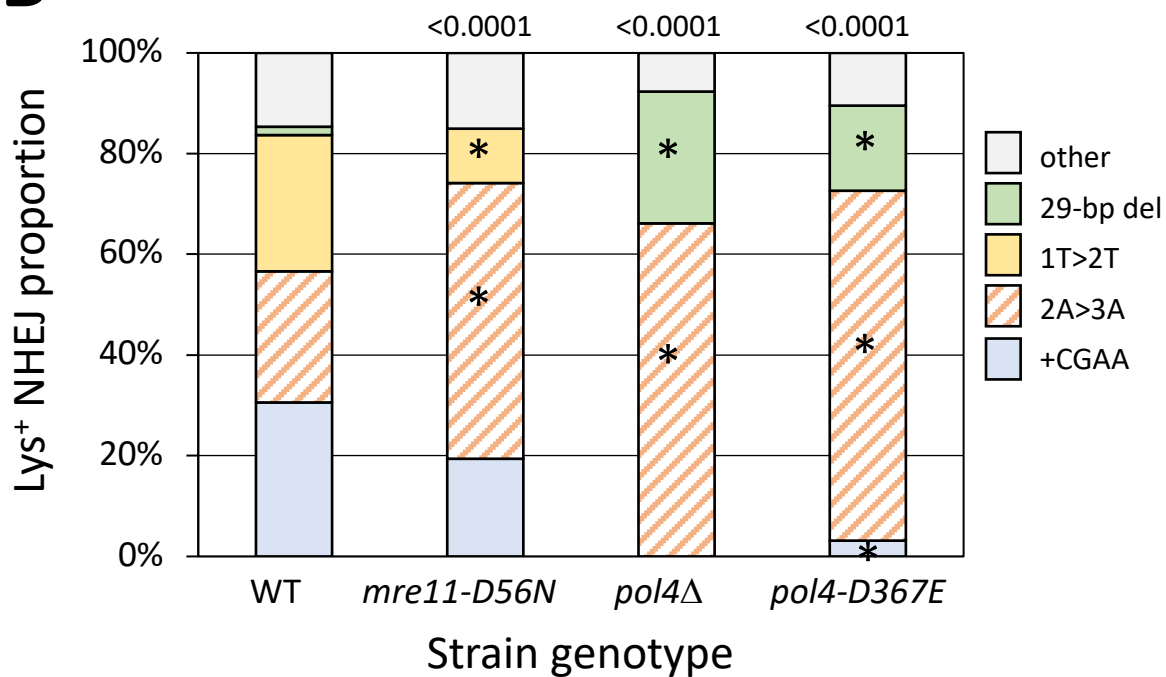
A**B**

Figure 3

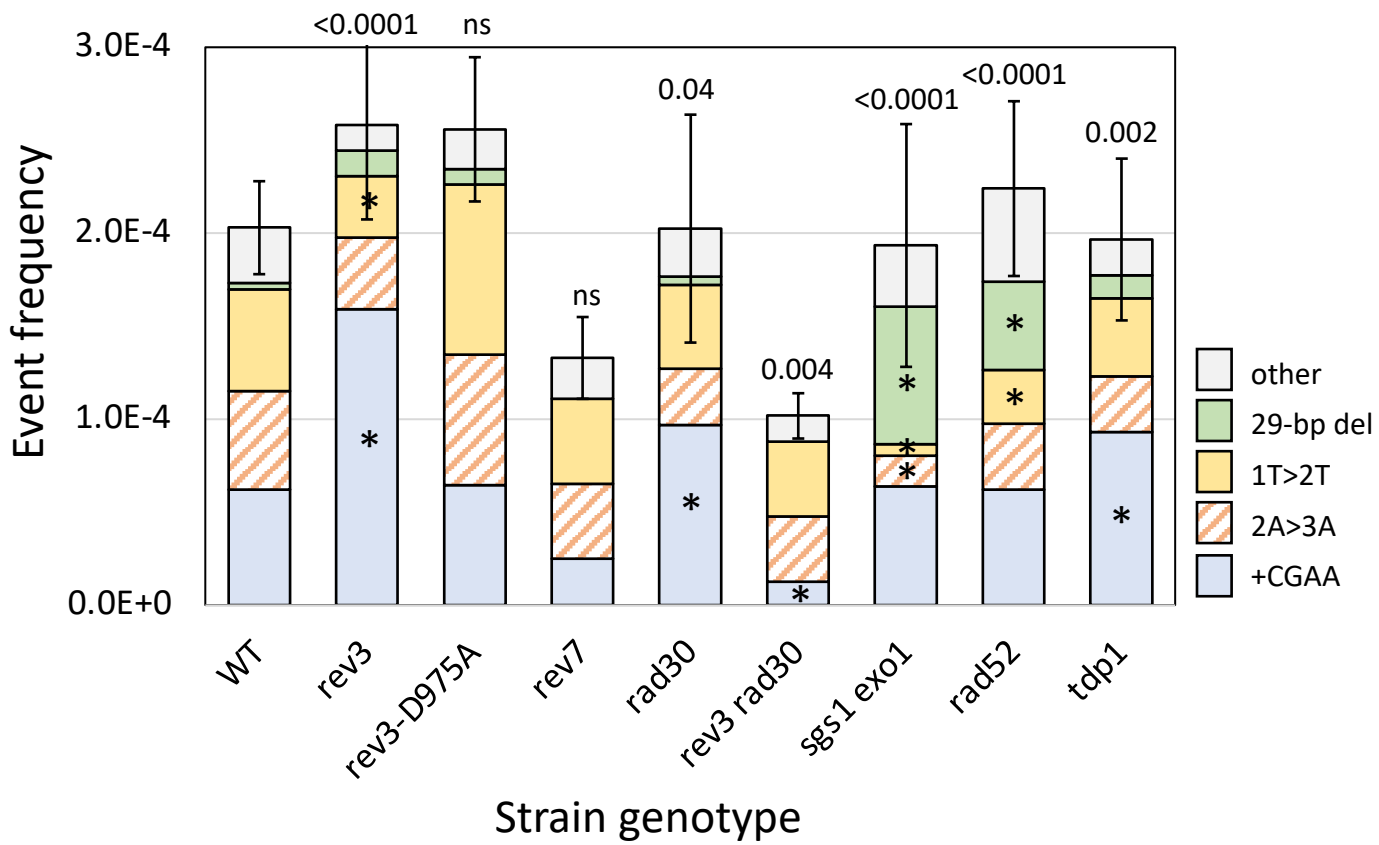
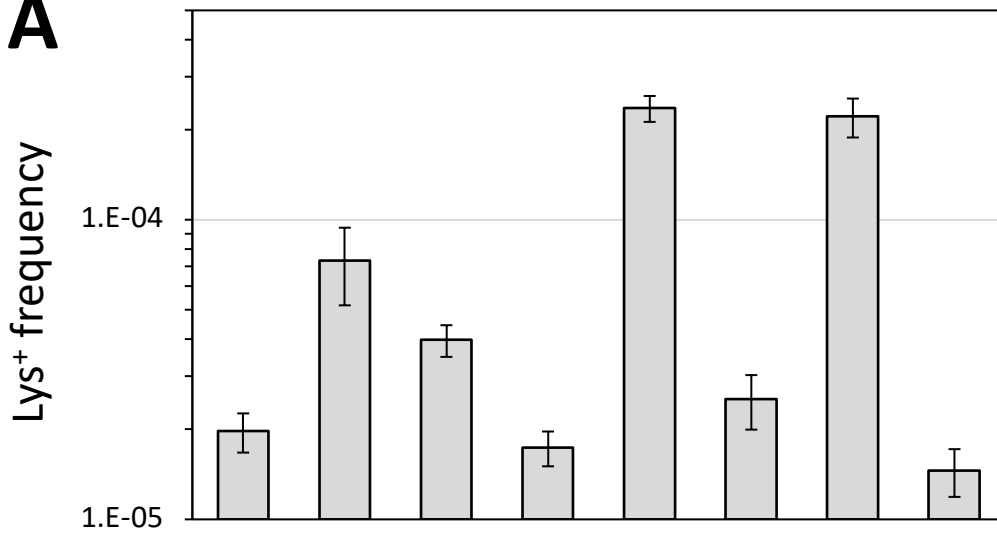
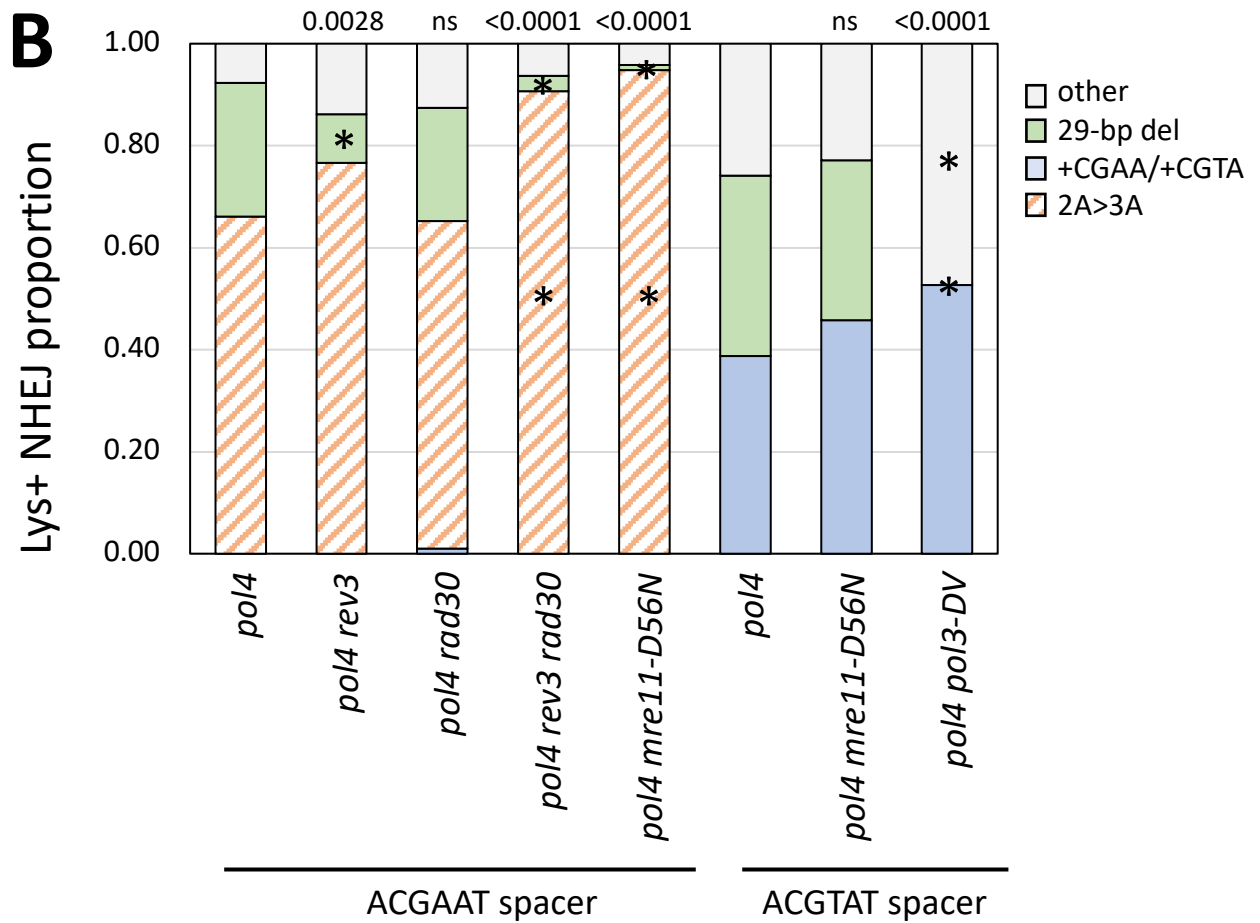


Figure 4

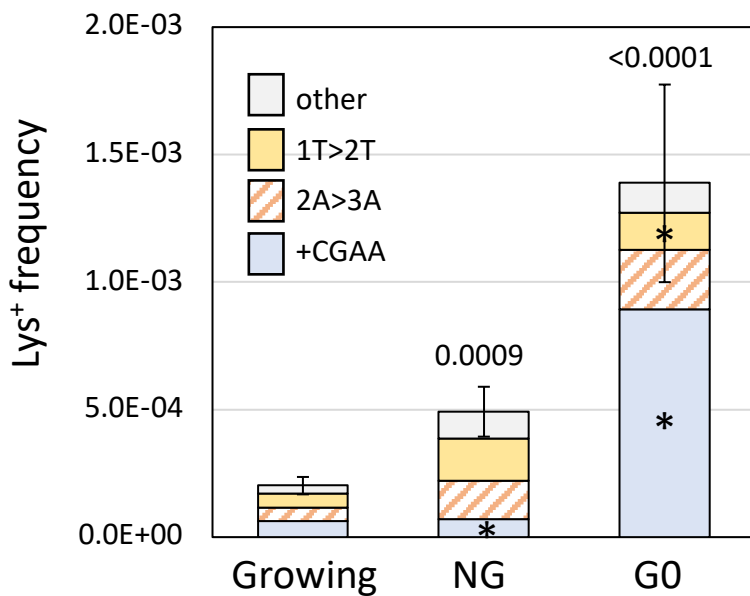
A



B



A



B

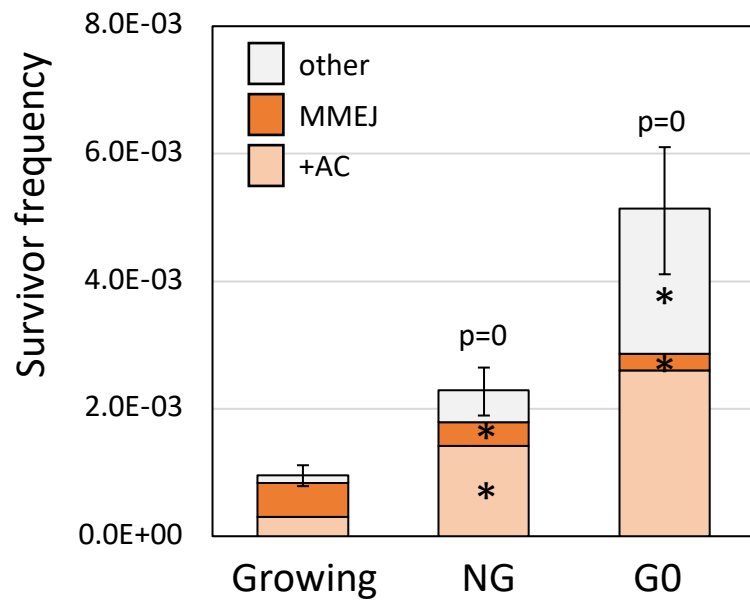


Table S1. Frequencies of Lys⁺ revertants and of survivors that lost the ZFN cleavage site

Spacer Sequence	Relevant Genotype	Lys ⁺ revertants		Survivors	
		Frequency x 10 ⁻⁴ (CI)	# of cultures	Frequency x 10 ⁻⁴ (CI)	# of cultures
ACGAAT	WT	2.03 (1.78-2.28)	47	9.53 (7.89-11.2)	113
	<i>ku70Δ</i>	ND	6	5.54 (3.98-7.18)	6
	<i>dnl4Δ</i>	ND	4	4.28 (3.08-5.56)	8
	<i>mre11Δ</i>	ND	12	1.65 (1.07-2.22)	12
	<i>mre11-D56N</i>	16.3 (14.2-18.4)	12	11.3 (8.72-14.1)	9
	<i>pol4Δ</i>	0.197 (0.167-0.226)	8	6.33 (4.28-8.45)	8
	<i>pol4-D367E</i>	0.417 (0.374-0.460)	16	5.53 (3.87-7.31)	16
	<i>pol4Δ mre11-D56N</i>	2.36 (2.12-2.59)	12	12.7 (10.0-15.2)	12
	<i>pol4Δ rad1Δ</i>	0.339 (0.301-0.377)	8	9.98 (4.26-16.5)	12
	<i>pol4Δ rev3Δ</i>	0.73 (0.519-0.942)	10	3.39 (2.09-4.74)	10
	<i>pol4Δ rad30Δ</i>	0.397 (0.349-0.445)	11		
	<i>pol4Δ rev3Δ rad30Δ</i>	0.174 (0.151-0.197)	10	6.89 (5.19-8.63)	10
	<i>rev3Δ</i>	2.58 (2.07-3.09)	11	11.5 (7.39-15.6)	11
	<i>rev3-D975A</i>	2.56 (2.17-2.95)	12	11.5 (7.71-15.2)	12
	<i>rev7Δ</i>	1.33 (1.12-1.55)	8	26.2 (14.6-37.4)	8
	<i>rad30Δ</i>	2.02 (1.41-2.64)	11	10.8 (7.72-13.8)	11
	<i>rev3Δ rad30Δ</i>	1.02 (0.897-1.14)	10	8.15 (5.10-11.2)	10
	<i>sgs1Δ exo1Δ</i>	1.93 (1.28-2.59)	10	0.579 (0.404-0.762)	14
	<i>rad52Δ</i>	2.24 (1.77-2.71)	10	1.43 (1.06-1.80)	20
	<i>tdp1Δ</i>	1.97 (1.53-2.40)	7	10.8 (8.22-13.5)	7
	<i>rad1Δ</i>	2.32 (1.66-2.99)	14	15.2 (9.19-21.0)	10
	<i>rad10Δ</i>	2.04 (1.65-2.42)	8	5.22 (4.00-6.35)	12
	<i>mus81Δ</i>	3.68 (2.50-4.86)	9	6.61 (4.93-8.40)	8
	<i>rad1Δ mus81Δ</i>	3.06 (1.97-4.15)	10	3.97 (3.05-4.83)	10
	<i>slx4Δ</i>	2.40	14	4.24	14

		(1.76-3.04)		(2.90-5.53)	
ACGTAT	<i>WT</i>	3.63 (3.12-4.13)	15		
	<i>mre11-D56N</i>	49.6 (32.9-66.2)	12		
	<i>pol4Δ</i>	0.252 (0.200-0.304)	12		
	<i>pol4Δ mre11-D56N</i>	2.21 (1.88-2.54)	12		
	<i>pol4Δ mre11Δ</i>	ND	12	1.10 (0.70-1.49)	12
	<i>pol4Δ pol3-D520V</i>	0.145 (0.119-0.172)	13	1.66 (0.98-2.60)	13

ND – None detected

Gray shading indicates that the strain was not analyzed

Table S2. Spectra in Lys+ revertants

SJR4848 (-1,ACGAAT) Lys+ revertants

Mutation	#	T	A	C	A						C	G	A	A				T				G	G	C	
+CGAA	69	T	A	C	A						C	G	A	A	C	G	A	A	T				G	G	C
2A>3A	59	T	A	C	A						C	G	A	A	A			T					G	G	C
1T>2T	61	T	A	C	A						C	G	A	A			T	T					G	G	C
1A>2A	14	T	A	C	A	A					C	G	A	A				T					G	G	C
1G>2G	5	T	A	C	A						C	G	G	A	A			T					G	G	C
1C>2C	4	T	A	C	A					C	C	G	A	A				T					G	G	C
2G>3G	1	T	A	C	A						C	G	A	A				T			G		G	G	C
+CGAACCC	1	T	A	C	A	C	G	A	A	C	C	C	C	C	C			T					G	G	C
+CGAATGG	1	T	A	C	A	C	G	A	A	T	G	G	G	G				T					G	G	C
+GAAT	1	T	A	C	A						C	G	A	A			T	G	A	A	T		G	G	C
-AC	1	T	A	C	-						-	G	A	A				T					G	G	C
-GAATG	2	T	A	C	A						C	-	-	-				-					-	G	C
-TGGCG	1	T	A	C	A						C	G	A	A				-					-	-	-
-23 bp	1	-	-	-	-						-	-	-	-				-					-	-	-
-29 bp	4	-	-	-	-						-	-	-	-				-					-	-	-
-56 bp	1	-	-	-	-						-	-	A	A			T					G	G	C	
TOTAL	226																								

None
GCC
AAT

SJR4883 (-1,ACGAAT) ku70Δ Lys+ revertants

SJR4880 (-1,ACGAAT) dni4Δ Lys+ revertants

SJR5247 (-1,ACGAAT) mre11Δ Lys+ revertants

SJR5223 (-1,ACGAAT) mre11-D56N Lys+ Revertants

Mutation	#	T	A	C	A						C	G	A	A				T	G	G	C			
+CGAA	18	T	A	C	A						C	G	A	A	C	G	A	A	T	G	G	C		
2A>3A	51	T	A	C	A						C	G	A	A	A			T	G	G	C			
1T>2T	10	T	A	C	A						C	G	A	A			T	T	G	G	C			
1A>2A	5	T	A	C	A	A					C	G	A	A				T	G	G	C			
1G>2G	3	T	A	C	A						C	G	G	A	A			T	G	G	C			
1C>2C	2	T	A	C	A					C	C	G	A	A				T	G	G	C			
+CGAATGG	1	T	A	C	A	C	G	A	A	T	G	G	G	G				T	G	G	C			
-AC	1	T	A	C	-						-	G	A	A				T	G	G	C			
-GAATG	1	T	A	C	A						C	-	-	-				-	-	-	G	C		
Complex Del	1	T	A	C	A						C	G	G	-	-			-	-	-	G	G	C	
TOTAL	93																							

SJR4876 (-1,ACGAAT) pol4Δ Lys+ Revertants

Mutation	#	T	A	C	A		C	G	A	A	T	G	G	C
2A>3A	121	T	A	C	A	C	G	A	A	A	T	G	G	C
1G>2G	3	T	A	C	A	C	G	G	A	A	T	G	G	C
2G>3G	1	T	A	C	A	C	G	A	A	T	G	G	G	C
1C>2C	1	T	A	C	A	C	C	G	A	A	T	G	G	C
-TGGCG	1	T	A	C	A	C	G	A	A	-	-	-	-	
-20 bp	1	-	-	-	-	-	-	A	A	T	G	G	C	
-29 bp	1	-	-	-	-	-	-	-	-	-	-	-	-	
-29 bp	48	-	-	-	-	-	-	-	-	-	-	-	-	
-50 bp	6	-	-	-	-	-	-	-	-	-	-	-	-	
TOTAL	183													

None
None
GCC
CCAAG

SJR5097 (-1,ACGAAT) pol4-D367E Lys+ Revertants

Mutation	#	T	A	C	A	C	G	A	A				T	G	G	C
+CGAA	3	T	A	C	A	C	G	A	A	C	G	A	A	T	G	C
2A>3A	66	T	A	C	A	C	G	A	A	A			T	G	C	
1G>2G	1	T	A	C	A	C	G	G	A	A			T	G	C	
2G>3G	2	T	A	C	A	C	G	A	A				T	G	C	
-TGGCG	1	T	A	C	A	C	G	A	A	-	-	-	-			
-14 bp	1	T	A	C	-	-	-	-	-	-	-	-	-			
-23 bp	1	-	-	-	-	-	-	-	-	-	-	-	-			
-29 bp	1	-	-	-	-	-	-	-	-	-	-	-	-			
-29 bp	1	-	-	-	-	-	-	-	-	-	-	-	-			
-29 bp	16	-	-	-	-	-	-	-	-	-	-	-	-			
-50 bp	2	-	-	-	-	-	-	-	-	-	-	-	-			

ACG
None
None
None
GCC
CCAAG

SJR5169 (-1,ACGAAT) pol4Δ mre11-D56N Lys+ Revertants

Mutation	#	T	A	C	A	C	G	A	A	T	G	G	C	
2A>3A	91	T	A	C	A	C	G	A	A	A	T	G	G	C
1G>2G	3	T	A	C	A	C	G	G	A	A	T	G	G	C
2G>3G	1	T	A	C	A	C	G	A	A	T	G	G	G	C
-29 bp	1	-	-	-	-	-	-	-	-	-	-	-	-	-
TOTAL	96													

GCC

SJR5196 (-1,ACGAAT) pol4Δrad1Δ Lys+ Revertants

Mutation	#	T	A	C	A	C	G	A	A	T	G	G	C	
2A>3A	80	T	A	C	A	C	G	A	A	A	T	G	G	C
1G>2G	2	T	A	C	A	C	G	G	A	A	T	G	G	C
2G>3G	1	T	A	C	A	C	G	A	A	T	G	G	G	C
+GAAT	1	T	A	C	A	C	G	A	A	T	G	A	A	T
-AC	1	T	A	C	-	-	G	A	A	T	-	-	-	-
-14 bp	1	T	A	C	-	-	-	-	-	-	-	-	-	-
-29 bp	7	-	-	-	-	-	-	-	-	-	-	-	-	-
-59 bp	1	-	-	-	-	-	-	-	-	-	-	-	-	-
-86 bp	1	-	-	-	-	-	-	-	-	-	-	-	-	-
TOTAL	95													

ACG

GCC

None

None

SJR52422 (-1,ACGAAT) pol4Δrev3Δ Lys+ Revertants

Mutation	#	T	A	C	A	C	G	A	A	T	G	G	C	
2A>3A	72	T	A	C	A	C	G	A	A	A	T	G	G	C
1G>2G	2	T	A	C	A	C	G	G	A	A	T	G	G	C
-CGTGG	1	T	A	C	A	C	G	A	A	T	G	G	-	
-29 bp	9	-	-	-	-	-	-	-	-	-	-	-	-	
-50 bp	4	-	-	-	-	-	-	-	-	-	-	-	-	
-74 bp	1	-	-	-	-	-	-	-	-	-	-	-	-	
-86 bp	2	-	-	-	-	-	-	-	-	-	-	-	-	
-95 bp	3	-	-	-	-	-	-	-	-	-	-	-	-	
TOTAL	94													

GCC

CCAAG

None

None

GACGAG

SJR4882 (-1,ACGAAT) pol4Δrad30Δ Lys+ Revertants

Mutation	#	T	A	C	A	C	G	A	A	T	G	G	C
+CGAA	1	T	A	C	A	C	G	A	A	C	G	A	A
2A>3A	61	T	A	C	A	-	-	C	G	A	A	A	T
1G>2G	5	T	A	C	A	-	-	C	G	G	A	A	T
-GA	1	T	A	C	A	-	-	C	-	-	A	T	G
-29 bp	21	-	-	-	-	-	-	-	-	-	-	-	-
-50 bp	5	-	-	-	-	-	-	-	-	-	-	-	-
-56 bp	1	-	-	-	-	-	-	-	-	A	A	T	G
TOTAL	95												

GCC

CCAAG

AAT

SJR4006 (-1,ACGAAT) pol4Δrev3Δrad30Δ Lys+ Revertants

Mutation	#	T	A	C	A	C	G	A	A	T	G	G	C	G	T
2A>3A	87	T	A	C	A	C	G	A	A	A	T	G	G	C	G
1G>2G	2	T	A	C	A	C	G	G	A	A	T	G	G	C	G
-TGGCG	1	T	A	C	A	C	G	A	A	-	-	-	-	-	T
-GT	1	T	A	C	A	C	G	A	A	T	G	G	C	-	-
-29 bp	1	-	-	-	-	-	-	-	-	-	-	-	-	-	-
-29 bp	3	-	-	-	-	-	-	-	-	-	-	-	-	-	-
-50 bp	1	-	-	-	-	-	-	-	-	-	-	-	-	-	-
TOTAL	96														

None

GCC

CCAAG

SJR4884 (-1,ACGAAT) rev3Δ Lys+ Revertants

Mutation	#	T	A	C	A	C	G	A	A	T	G	G	C
+CGAA	58	T	A	C	A	C	G	A	A	C	G	A	A
2A>3A	14	T	A	C	A	C	G	A	A	A	T	G	G
1T>2T	12	T	A	C	A	C	G	A	A	-	T	T	G
1A>2A	3	T	A	C	A	A	C	G	A	A	-	T	G
1G>2G	2	T	A	C	A	C	G	G	A	A	T	G	G
-29 bp	5	-	-	-	-	-	-	-	-	-	-	-	-
TOTAL	94												

GCC

SJR5098 (-1,ACGAAT) rev3-D975A Lys+ Revertants

Mutation	#	T	A	C	A	C	G	A	A	T	G	G	C
----------	---	---	---	---	---	---	---	---	---	---	---	---	---

SJR5201 (-1,ACGAAT) mus81Δ Lys+ Revertants

Mutation	#	T	A	C	A	C	G	A	A	T	G	G	C
+CGAA	28	T	A	C	A	C	G	A	A	C	G	A	A
2A>3A	10	T	A	C	A	C	G	A	A	A	T	G	G
1T>2T	39	T	A	C	A	C	G	A	A	T	T	G	G
1A>2A	7	T	A	C	A	A	C	G	A	A	T	G	G
2G>3G	1	T	A	C	A	C	G	A	A	T	G	G	G
1G>2G	1	T	A	C	A	C	G	G	A	A	T	G	G
1C>2C	1	T	A	C	A	C	G	A	A	T	G	G	C
+CAAA	1	T	A	C	A	C	G	A	A	C	A	A	A
-CA	2	T	A	-	-	C	G	A	A	T	G	G	C
Complex Del	1	T	A	C	A	C	G	A	A	C	-	-	C
TOTAL	91												

SJR5202 (-1,ACGAAT) mus81Δrad1Δ Lys+ Revertants

Mutation	#	T	A	C	A	C	G	A	A	T	G	G	C
+CGAA	39	T	A	C	A	C	G	A	A	C	G	A	A
2A>3A	13	T	A	C	A	C	G	A	A	A	T	G	G
1T>2T	31	T	A	C	A	C	G	A	A	T	T	G	G
1A>2A	3	T	A	C	A	A	C	G	A	A	T	G	G
2G>3G	1	T	A	C	A	C	G	A	A	T	G	G	G
1G>2G	2	T	A	C	A	C	G	G	A	A	T	G	G
1C>2C	1	T	A	C	A	C	G	A	A	T	G	G	C
-GC	1	T	A	C	A	C	G	A	A	T	G	-	-
-CA	1	T	A	-	-	C	G	A	A	T	G	G	C
-29 bp	1	-	-	-	-	-	-	-	-	-	-	-	-
-50 bp	1	-	-	-	-	-	-	-	-	-	-	-	-
TOTAL	94												

GCC
CCAAG

SJR5240 (-1,ACGAAT) slx4Δ Lys+ Revertants

Mutation	#	T	A	C	A	C	G	A	A	T	G	G	C
+CGAA	37	T	A	C	A	C	G	A	A	C	G	A	A
2A>3A	32	T	A	C	A	C	G	A	A	A	T	G	G
1T>2T	18	T	A	C	A	C	G	A	A	T	T	G	G
1A>2A	3	T	A	C	A	A	C	G	A	A	T	G	G
1G>2G	2	T	A	C	A	C	G	G	A	A	T	G	G
1C>2C	1	T	A	C	A	C	G	A	A	T	G	G	C
+TTTT	1	T	A	C	A	C	G	A	A	T	T	T	T
-GA	1	T	A	C	A	C	-	-	A	T	G	G	C
-29 bp	7	-	-	-	-	-	-	-	-	-	-	-	-
-35 bp	1	-	-	-	-	-	-	-	-	-	-	-	-
-50 bp	1	-	-	-	-	-	-	-	-	-	-	-	-
-53 bp (Complex)	1	-	-	-	-	-	-	-	-	-	-	-	-
-74 bp	1	-	-	-	-	-	-	-	-	-	-	-	-
-95 bp	2	-	-	-	-	-	-	-	-	-	-	-	-
TOTAL	108												

GCC
GTT
CCAAG
None
None
GACGAG

SJR5224 (-1,ACGTAT) Lys+ Revertants

Mutation	#	T	A	C	A	C	G	T	A	T	G	G	C
+CGTA	43	T	A	C	A	C	G	T	A	C	G	T	A
+CGTC	1	T	A	C	A	C	G	T	C	C	G	T	A
+CGTAAAA	1	T	A	C	A	C	G	T	A	A	A	A	A
1C>2C	3	T	A	C	A	C	G	T	A	T	G	G	C
1T>2T	63	T	A	C	A	C	G	T	A	T	T	G	G
-AT	1	T	A	C	A	C	G	T	-	-	G	G	C
-TG	1	T	A	C	A	C	G	T	A	-	-	G	C
-AC	1	T	A	C	-	-	G	T	A	T	G	G	C
-29 bp	2	-	-	-	-	-	-	-	-	-	-	-	-
TOTAL	116												

GCC

SJR5227 (-1,ACGTAT) mre11-D56N Lys+ Revertants

Mutation	#	T	A	C	A	C	G	T	A	T	G	G	C
+CGTA	73	T	A	C	A	C	G	T	A	C	G	T	A
1C>2C	1	T	A	C	A	C	G	T	A	T	G	G	C
1T>2T	14	T	A	C	A	C	G	T	A	T	T	G	G
Complex Del	1	T	A	C	A	C	G	T	A	T	A	-	-
-AT	4	T	A	C	A	C	G	T	-	-	G	G	C
-CG	1	T	A	C	A	-	-	T	A	T	G	G	C
-TG	1	T	A	C	A	C	G	T	A	-	-	G	C

Table S3. Spectra in survivors

SJR4848 (-1,ACGAAT) Survivors

Mutation	#	T	A	C	A	C	G	A	A	T	G	G	C
+AC	26	T	A	C	A	C	G	A	A	T	G	G	C
+CGAAC	1	T	A	C	A	C	G	A	A	C	G	A	A
+CGA	1	T	A	C	A	C	G	A	A	T	G	G	C
+AA	1	T	A	C	A	A	A	A	A	T	G	G	C
+AA	1	T	A	C	A	A	A	A	A	T	G	G	C
+AAAA	1	T	A	C	A	A	A	A	A	T	G	G	C
-A	1	T	A	C	-	-	-	-	-	T	G	G	C
-A	1	T	A	C	A	-	-	-	-	T	G	G	C
-37 bp	1	T	A	C	A	-	-	-	-	-	-	-	-
-19 bp	1	-	-	-	-	-	-	-	-	T	G	G	C
-15 bp	1	-	-	-	-	-	-	-	-	-	G	C	
-1175 bp	36	T	A	C	A	-	-	-	-	-	-	-	-
-11,731 bp	11	-	-	-	-	-	-	-	-	-	-	-	-
Maintain Cut Site	72	T	A	C	A	-	-	-	-	T	G	G	C
TOTAL sequenced	155												

None
None
None
CCAAGCTACTACA
TGGAAAAAAAAAAAA

SJR4883 (-1,ACGAAT) ku70Δ Survivors

Mutation	#	T	A	C	A	C	G	A	A	T	G	G	C
-1175 bp	35	T	A	C	A	-	-	-	-	-	-	-	-
-11,731 bp	3	-	-	-	-	-	-	-	-	-	-	-	-
Maintain Cut Site	56	T	A	C	A	C	G	A	A	T	G	G	C
TOTAL sequenced	94												

CCAAGCTACTACA
TGGAAAAAAAAAAAA

SJR4880 (-1,ACGAAT) dnl4Δ Survivors

Mutation	#	T	A	C	A	C	G	A	A	T	G	G	C
-1175 bp	24	T	A	C	A	-	-	-	-	-	-	-	-
-11,731 bp	14	-	-	-	-	-	-	-	-	-	-	-	-
Maintain Cut Site	58	T	A	C	A	C	G	A	A	T	G	G	C
TOTAL sequenced	96												

CCAAGCTACTACA
TGGAAAAAAAAAAAA

SJR5247 (-1,ACGAAT) mre11Δ Survivors

Mutation	#	T	A	C	A	C	G	A	A	T	G	G	C
-1175 bp	46	T	A	C	A	-	-	-	-	-	-	-	-
-11,731 bp	1	-	-	-	-	-	-	-	-	-	-	-	-
Maintain Cut Site	47	T	A	C	A	C	G	A	A	T	G	G	C
TOTAL sequenced	94												

CCAAGCTACTACA
TGGAAAAAAAAAAAA

SJR5223 (-1,ACGAAT) mre11-D56N Survivors

Mutation	#	T	A	C	A	C	G	A	A	T	G	G	C
+AC	7	T	A	C	A	C	G	A	A	T	G	G	C
+CGAA	1	T	A	C	A	C	G	A	A	C	G	A	A
2A>3A	8	T	A	C	A	C	G	A	A	A	T	G	C
+AA	2	T	A	C	A	C	G	A	A	A	A	T	C
-A	1	T	A	C	A	C	G	A	-	T	G	G	C
-1175 bp	29	T	A	C	A	-	-	-	-	-	-	-	-
-11,731 bp	5	-	-	-	-	-	-	-	-	-	-	-	-
Maintain Cut Site	34	T	A	C	A	C	G	A	A	T	G	G	C
TOTAL sequenced	87												

CCAAGCTACTACA
TGGAAAAAAAAAAAA

SJR4876 (-1,ACGAAT) pol4Δ Survivors

Mutation	#	T	A	C	A	C	G	A	A	T	G	G	C
2A>3A	2	T	A	C	A	C	G	A	A	A	T	G	C
-1175 bp	29	T	A	C	A	-	-	-	-	-	-	-	-
-11,731 bp	8	-	-	-	-	-	-	-	-	-	-	-	-
Maintain Cut Site	54	T	A	C	A	C	G	A	A	T	G	G	C
TOTAL sequenced	93												

CCAAGCTACTACA
TGGAAAAAAAAAAAA

SJR5097 (-1,ACGAAT) pol4-D367E Survivors

Mutation	#	T	A	C	A	C	G	A	A	T	G	G	C
-1175 bp	32	T	A	C	A	-	-	-	-	-	-	-	-
-11,731 bp	2	-	-	-	-	-	-	-	-	-	-	-	-
Maintain Cut Site	62	T	A	C	A	C	G	A	A	T	G	G	C
TOTAL sequenced	96												

CCAAGCTACTACA
TGGAAAAAAAAAAAA

SJR5169 (-1,ACGAAT) pol4Δ mre11-D56N Survivors

Mutation	#	T	A	C	A	C	G	A	A	T	G	G	C
+CACGAA	1	T	A	C	A	C	A	C	G	A	A	C	G
2A>3A	10	T	A	C	A	-	-	-	-	C	G	A	A
+GA	1	T	A	C	A	-	-	-	-	C	G	A	A
-55 bp	1	T	A	C	-	-	-	-	-	-	-	-	-
-1175 bp	42	T	A	C	A	-	-	-	-	-	-	-	-
-11,731 bp	8	-	-	-	-	-	-	-	-	-	-	-	-
Maintain Cut Site	33	T	A	C	A	-	-	-	-	C	G	A	A
TOTAL sequenced	96												

ACGA
CCAAGCTACTACA
TGGAAAAAAAAAAAA

SJR5196 (-1,ACGAAT) pol4Δrad1Δ Survivors

Mutation	#	T	A	C	A	C	G	A	A	T	G	G	C
-55 bp	2	T	A	C	-	-	-	-	-	-	-	-	-
-231 bp	1	T	A	C	-	-	-	-	-	-	-	-	-

ACGA
None

-1175 bp	38	T A C A C G A A T G G C
-11,731 bp	32	T A C A C G A A T G G C
Maintain Cut Site	17	T A C A C G A A T G G C
TOTAL sequenced	90	

SJR5242 (-1,ACGAAT) pol4Δrev3Δ Survivors

Mutation	#	T A C A C G A A T G G C	ACGA GAA None CCAAGCTACTACA TGGAAAAAAAAAAAA
2A>3A	2	T A C A C G A A A T G G C	
-55 bp	1	T A C - - - - -	
-154 bp	1	T A C A C - - - - -	
-231 bp	1	T A C - - - - -	
-1175 bp	20	T A C A - - - - -	
-11,731 bp	10	- - - - -	
Maintain Cut Site	55	T A C A C G A A T G G C	
TOTAL sequenced	90		

SJR4882 (-1,ACGAAT) pol4Δrad30Δ Survivors

SJR4006 (-1,ACGAAT) pol4Δrev3Δrad30Δ Survivors

Mutation	#	T A C A C G A A T G G C	CCAAGCTACTACA TGGAAAAAAAAAAAA
2A>3A	2	T A C A C G A A A T G G C	
-A	2	T A C A C G A - T G G C	
-1175 bp	29	T A C A - - - - -	
-11,731 bp	10	- - - - -	
Maintain Cut Site	50	T A C A C G A A T G G C	
TOTAL sequenced	93		

SJR4884 (-1,ACGAAT) rev3Δ Survivors

Mutation	#	T A C A C G A A T G G C	CCAAGCTACTACA TGGAAAAAAAAAAAA
+AC	14	T A C A C A C G A A T G G C	
+CGAA	1	T A C A C A C G A A C G A A T G G C	
2A>3A	1	T A C A C A C G A A A T G G C	
+AA	1	T A C A A A C G A A T G G C	
-A	1	T A C A C G A - T G G C	
-1175 bp	22	T A C A - - - - -	
-11,731 bp	12	- - - - -	
Maintain Cut Site	39	T A C A C G A A T G G C	
TOTAL sequenced	91		

SJR5098 (-1,ACGAAT) rev3-D975A Survivors

Mutation	#	T A C A C G A A T G G C	CCAAGCTACTACA TGGAAAAAAAAAAAA
+AC	13	T A C A C A C G A A T G G C	
2A>3A	5	T A C A C A C G A A A T G G C	
+GAA	1	T A C A C A C G A A G A A T G G C	
+TT	1	T A C A C A C G A A T T T G G C	
-1175 bp	20	T A C A - - - - -	
-11,731 bp	6	- - - - -	
Maintain Cut Site	46	T A C A C G A A T G G C	
TOTAL sequenced	92		

SJR5193 (-1,ACGAAT) rev7Δ Survivors

Mutation	#	T A C T A C A C G A A T G G C	CCAAGCTACTACA TGGAAAAAAAAAAAA
+AC	6	T A C T A C A C A C G A A T G G C	
+CGAAAA	1	T A C T A C A C A C G A A A A A C G A A T G G C	
+CGAAAA	1	T A C T A C A C A C G A A A A A C G A A T G G C	
+CGAAT	1	T A C T A C A C A C G A A T C G A A T G G C	
+CGAAA	1	T A C T A C A C A C G A A A C G A A T G G C	
+CGAA	1	T A C T A C A C A C G A A C G A A T G G C	
+CGA	2	T A C T A C A C A C G A C G A A T G G C	
+CGG	1	T A C T A C A C A C G G C G A A T G G C	
+TT	1	T A C T A C A C A C G A A T T T G G C	
+GAA	1	T A C T A C A C A C G A A G A A T G G C	
+AAA	1	T A C T A C A C A C G A A A A A T G G C	
+AAAA	1	T A C T A C A C A C G A A A A A A T G G C	
+CCCGAA	1	T A C T A C A C A C G A A C C C G A A T G G C	
2A>3A	3	T A C T A C A C A C G A A A T G G C	
1C>2C	1	T A C T A C A C A C G A A T G G C	
1G>2G	1	T A C T A C A C A C G G A A T G G C	
1T>2T	1	T A C T A C A C A C G A A T T G G C	
-CG	1	T A C T A C A C A C G A A T G G C	
-AGCT	1	- A C T A C A C G A A T G G C	
-1175 bp	25	T A C T A C A C A C G A A T G G C	
-11,731 bp	18	- - - - -	
Maintain Cut Site	21	T A C T A C A C A C G A A T G G C	
TOTAL sequenced	91		

SJR4963 (-1,ACGAAT) rad30Δ Survivors

Mutation	#	T A C A C G A A T G G C	None CCAAGCTACTACA TGGAAAAAAAAAAAA
+AC	14	T A C A C A C G A A T G G C	
+CGAAA	1	T A C A C A C G A A A C G A A T G G C	
-A	1	T A C A C G A - T G G C	
-231 bp	1	T A C A C - - - - -	
-1175 bp	25	T A C A C A - - - - -	
-11,731 bp	11	- - - - -	

Maintain Cut Site	38
TOTAL sequenced	91

SJR4964 (-1,ACGAAT) rev3Δrad30Δ Survivors

Mutation	#	T	A	C	A	C	G	A	A	T	G	G	C
+AC	12	T	A	C	A	C	G	A	A	T	G	G	C
2A>3A	1	T	A	C	A	C	G	A	A	A	T	G	C
-A	1	T	A	C	A	C	G	A	-	T	G	G	C
-751 bp	1	T	A	C	A	-	-	-	-	-	-	-	-
-1175 bp	22	T	A	C	A	-	-	-	-	-	-	-	-
-11,731 bp	11	-	-	-	-	-	-	-	-	-	-	-	-
Maintain Cut Site	48	T	A	C	A	C	G	A	A	T	G	G	C
TOTAL sequenced	96												

None
 CCAAGCTACTACA
 TGGAAAAAAAAAAAA

SJR5013 (-1,ACGAAT) sgs1Δexo1Δ Survivors

Mutation	#	A	G	C	T	A	C	T	A	C	A	A	C	G	A	A	T	G	G	C						
+AC	24	A	G	C	T	A	C	T	A	C	A	A	C	G	A	A	T	G	G	C						
+CGAACCC	1	A	G	C	T	A	C	T	A	C	A	C	G	A	A	C	C	C	C	G	A	A	T	G	G	C
+CGAA	5	A	G	C	T	A	C	T	A	C	A	C	G	A	A	C	G	A	A	T	G	G	C			
+CGA	1	A	G	C	T	A	C	T	A	C	A	C	G	A	A	C	G	A	A	T	G	G	C			
+CG	1	A	G	C	T	A	C	T	A	C	A	C	G	A	A	C	G	A	A	T	G	G	C			
+GAA	1	A	G	C	T	A	C	T	A	C	A	A	C	G	A	A	G	A	A	T	G	G	C			
-29 bp	1	-	-	-	-	-	-	-	-	-	-	-	-	-	-	-	-	-	-	-	-	-	-	-		
-75 bp	1	-	-	-	-	-	-	-	-	-	-	-	-	-	-	-	-	-	-	-	-	-	-	-		
-231 bp	1	A	G	C	T	A	C	T	A	C	A	A	C	G	A	A	T	G	G	C						
-1175 bp	2	A	G	C	T	A	C	T	A	C	A	A	C	G	A	A	T	G	G	C						
-1384 bp	1	A	-	-	-	-	-	-	-	-	-	-	-	-	-	-	-	-	-	-	-	-	-	-		
Maintain Cut Site	52	A	G	C	T	A	C	T	A	C	A	A	C	G	A	A	T	G	G	C						
TOTAL sequenced	91																									

GCC
 AGTT
 None
 CCAAGCTACTACA
 None

SJR5194 (-1,ACGAAT) rad52Δ Survivors

Mutation	#	T	A	C	A	C	G	A	A	T	G	G	C
+AC	36	T	A	C	A	C	G	A	A	T	G	G	C
2A>3A	2	T	A	C	A	C	G	A	A	A	T	G	C
+AA	1	T	A	C	A	C	G	A	A	A	T	G	C
-1175 bp	18	T	A	C	A	-	-	-	-	-	-	-	-
-11,731 bp	1	-	-	-	-	-	-	-	-	-	-	-	-
Maintain Cut Site	65	T	A	C	A	C	G	A	A	T	G	G	C
TOTAL sequenced	123												

CCAAGCTACTACA
 TGGAAAAAAAAAAAA

SJR4885 (-1,ACGAAT) tdp1Δ Survivors

Mutation	#	T	A	C	A	C	G	A	A	T	G	G	C
+AC	12	T	A	C	A	C	G	A	A	T	G	G	C
2A>3A	2	T	A	C	A	C	G	A	A	A	T	G	C
-A	1	T	A	C	A	C	G	A	-	T	G	G	C
-56 bp	1	-	-	-	-	-	-	-	A	A	T	G	C
-75 bp	1	T	A	C	A	-	-	-	-	-	-	-	-
-1175 bp	28	T	A	C	A	-	-	-	-	-	-	-	-
-11,731 bp	14	-	-	-	-	-	-	-	-	-	-	-	-
Maintain Cut Site	51	T	A	C	A	C	G	A	A	T	G	G	C
TOTAL sequenced	110												

ATT
 None
 CCAAGCTACTACA
 TGGAAAAAAAAAAAA

SJR5199 (-1,ACGAAT) rad1Δ Survivors

Mutation	#	T	A	C	A	C	G	A	A	T	G	G	C
+AC	33	T	A	C	A	C	G	A	A	T	G	G	C
1A>2A	1	T	A	C	A	C	G	A	A	T	G	G	C
2A>3A	3	T	A	C	A	C	G	A	A	A	T	G	C
1T>2T	1	T	A	C	A	C	G	A	A	T	T	G	C
1G>2G	1	T	A	C	A	C	G	G	A	A	T	G	C
-A	4	T	A	C	A	C	G	A	-	T	G	G	C
-1175 bp	28	T	A	C	A	-	-	-	-	-	-	-	-
-11,731 bp	9	-	-	-	-	-	-	-	-	-	-	-	-
Maintain Cut Site	5	T	A	C	A	C	G	A	A	T	G	G	C
TOTAL sequenced	85												

CCAAGCTACTACA
 TGGAAAAAAAAAAAA

SJR5200 (-1,ACGAAT) rad10Δ Survivors combined

Mutation	#	T	A	C	A	C	G	A	A	T	G	G	C
+AC	58	T	A	C	A	C	G	A	A	T	G	G	C
+AA	1	T	A	C	A	A	A	C	G	A	A	T	G
1G>2G	1	T	A	C	A	C	G	G	A	A	T	G	C
1T>2T	1	T	A	C	A	C	G	A	A	T	T	G	C
2A>3A	5	T	A	C	A	C	G	A	A	A	T	G	C
+CGAAC	1	T	A	C	A	C	G	A	A	C	G	A	T
+CGAA	2	T	A	C	A	C	G	A	A	C	G	A	T
+GAAT	1	T	A	C	A	C	G	A	A	T	G	A	T
+GGAAT	1	T	A	C	A	C	G	A	A	T	G	G	A
-A	4	T	A	C	A	C	G	A	-	T	G	G	C
-43 bp	1	-	-	-	-	-	-	-	G	A	A	T	G
-56 bp	1	-	-	-	-	-	-	-	A	A	T	G	C
-1175 bp	55	T	A	C	A	-	-	-	-	-	-	-	-
-11,731 bp	17	-	-	-	-	-	-	-	-	-	-	-	-
Maintain Cut Site	31	T	A	C	A	C	G	A	A	T	G	G	C
TOTAL sequenced	180												

None
 AAT
 CCAAGCTACTACA
 TGGAAAAAAAAAAAA

Mutation	#	T	A	C		A	C	G	A	A	T	G	G	C
+AC	16	T	A	C		A	C	G	A	A	T	G	G	C
-1175 bp	18	T	A	C		A	-	-	-	-	-	-	-	-
-11,731 bp	6	-	-	-		-	-	-	-	-	-	-	-	-
Maintain Cut Site	55	T	A	C		A	C	G	A	A	T	G	G	C
TOTAL sequenced	95													

CCAAGCTACTACA
TGGAAAAAAAAAAAA

SJR5202 (-1,ACGAAT) mus81Δrad1Δ Survivors

Mutation	#	T	A	C		A				C	G	A	A	T	G	G	C	
+AC	24	T	A	C		A				C	G	A	A	T	G	G	C	
+CGAA	4	T	A	C		A	C	G	A	A	C	G	A	A	T	G	G	C
2A>3A	1	T	A	C		A				C	G	A	A	A	T	G	G	C
-A	2	T	A	C		A				C	G	A	-	T	G	G	C	
-1175 bp	26	T	A	C		A				-	-	-	-	-	-	-	-	
-11,731 bp	7	-	-	-		-				-	-	-	-	-	-	-	-	
Maintain Cut Site	22	T	A	C		A				C	G	A	A	T	G	G	C	
TOTAL sequenced	86																	

CCAAGCTACTACA
TGGAAAAAAAAAAAA

SJR5240 (-1,ACGAAT) slx4Δ Survivors

Mutation	#	T	A	C				A	C					G	A	A			T	G	G	C		
+AC	32	T	A	C				A	C					G	A	A			T	G	G	C		
+CGAA	1	T	A	C				A	C					G	A	A	C	G	A	A	T	G	G	C
2A>3A	2	T	A	C				A	C					G	A	A	A		T	G	G	C		
+GAATG	1	T	A	C				A	C	G	A	A	T	G	G	A	A		T	G	G	C		
+CGAAA	1	T	A	C				C	G	A	A	A	A	C					T	G	G	C		
-A	1	T	A	C				A	C					G	A	-			T	G	G	C		
-CTA	1	-	-	C				A	C					G	A	A			T	G	G	C		
-1175 bp	32	T	A	C				A	-					-	-	-			-	-	-	-		
-11,731 bp	0	-	-	-				-	-					-	-	-			-	-	-	-		
Maintain Cut Site	18	T	A	C				A	C					G	A	A			T	G	G	C		
TOTAL sequenced	89																							

CCAAGCTACTACA
TGGAAAAAAAAAAAA

SJR5224 (-1,ACGTAT) Survivors

SJR5227 (-1,ACGTAT) mre11-D56N Survivors

SJR5225 (-1,ACGTAT) pol4Δ Survivors

SJR5226 (-1,ACGTAT) pol4Δ mre11-D56N Survivors

SJR5248 (-1,ACGTAT) pol4Δmre11Δ Survivors

Mutation	#	T	A	C	A	C	G	T	A	T	G	G	C
-1175 bp	45	T	A	C	A	-	-	-	-	-	-	-	-
-11,731 bp	0	-	-	-	-	-	-	-	-	-	-	-	-
Maintain Cut Site	43	T	A	C	A	C	G	T	A	T	G	G	C
TOTAL sequenced	88												

CCAAGCTACTACA
TGGAAAAAAAAAAAA

SJR5241 (-1,ACGTAT) pol4Δ pol3-DV Survivors

Mutation	#	T	A	C	A	C	G	T	A	T	G	G	C
Complex Insertion	1	T	A	C	A	C	G	T	A	T	G	G	C
-1175 bp	11	T	A	C	A	-	-	-	-	-	-	-	-
-11,731 bp	3	-	-	-	-	-	-	-	-	-	-	-	-
Maintain Cut Site	81	T	A	C	A	C	G	T	A	T	G	G	C
TOTAL sequenced	96												

CCAAGCTACTACA
TGGAAAAAAAAAAAA